12-2016

Analytical Study of Miniature Thermoelectric Device

Mohammed Dhannoon
Western Michigan University

ANALYTICAL STUDY OF MINIATURE THERMOELECTRIC DEVICE

by

Mohammed Dhannoon

A thesis submitted to the Graduate College
in partial fulfillment of the requirements for the degree of
Master of Science in Engineering (Mechanical)
Mechanical and Aerospace Engineering
Western Michigan University
December 2016

Thesis Committee:

HoSung Lee, Ph.D., Chair
Christopher Cho, Ph.D.
Muralidhar Ghantasala, Ph.D.

ANALYTICAL STUDY OF MINIATURE THERMOELECTRIC DEVICES

Mohammed Dhannoon, M.S.E.

Western Michigan University, 2016

Miniature thermoelectric devices (TE) have been regarded as hopeful devices to attain efficient cooling in microprocessors and other small-scale devices. To recognize the performances of miniature thermoelectric coolers, a thermoelectric cooling module is theoretically analyzed. Particular attention is paid to the impact of the thermoelectric element length effect and the substrate material type influence on the cooling performance. The electrical contact resistance and thermal contact are taken into account.

Furthermore, miniature thermoelectric is compared with large thermoelectric, and effective material properties of miniature thermoelectric are studied. The obtained results also demonstrate power density (cooling/heating power per unit area of the device) of thermoelectric with miniature thermoelectric can be improved, where power density of μTEC is 15 W/cm^2 compared with large TEC 0.37 W/cm^2.

ACKNOWLEDGEMENTS

Foremost I would like to thank my thesis advisor, Dr. HoSung Lee at Western Michigan University. Prof. Lee's office was constantly open when I drove into a problem or had a question about my thesis or writing. He steered me in the right the direction whenever he thought I needed it.

I would also like to thank the experts who were the committee members for this research project: Dr. Cristopher Cho, and Muralidhar Ghantasala of the experts who contributed. Without their passionate participation and their guide, the work could not have been successfully conducted.

Ultimately, I must express my very sincere appreciation to my parents and my spouse for granting me with surefire support and constant encouragement during my years of study and through the process of researching and writing this research. This attainment would not have been achievable without them.

Mohammed Dhannoon

TABLE OF CONTENTS

Table of Contents—Continued

CHAPTER

Table of Contents—Continued

LIST OF TABLES

LIST OF FIGURES

List of Figures—Continued

List of Figures—Continued

CHAPTER I

1 INTRODUCTION AND BACKGROUND

The process of conversion of electrical energy to thermal energy or vice-versa is called the thermoelectric phenomena. The studies, researches, and developments of TE devices have gotten a good deal of attention due to the practical applications in green energy of the thermoelectric devices [1]. The thermoelectric devices can be divided into two different types: one, a thermoelectric generator (TEG), and the other, a thermoelectric cooler (TEC). The former occurs when the device operates as an energy-generating device (converting thermal energy to electrical energy by Seebeck impact [2]). The source of thermal energy manifests itself as a temperature difference across a TEG [3]. The later occurs when the device operates in a cooling or heating way (converting electrical energy to thermal energy by Peltier effect [2, 4, and 5]). The sources of heating or cooling form a heat flux that produces or causes a temperature variation across a thermoelectric cooler.

The thermoelectric devices have many advantages, such as solid-state mechanism, no moving parts, easily controlled by electric power, and decreasing their susceptibility to mechanical breakdown while permitting to extend periods of operation with lower maintenance. Furthermore, these advantages make cooling operations operate with no noise, compared to traditional refrigeration operations, and there are no pollutants or

environmentally harmful byproducts [3, 6]. Thermoelectric devices are used in many applications because of these advantages.

The applications of thermoelectric generator devices are used in automotive vehicles as exhaust waste heat-recovery devices, where thermal energy is scavenged along the exhaust line of a vehicle and changed into helpful electricity [7]. TEGs are used in exploration robot's rover in space in order to produce electricity energy from heat energy liberated from the decay of radioisotopes [8]. Also, sunlight can be utilized to generate energy as electricity by using STEG that absorb sunlight and implement the conversion process [9, 10].

1.1 Thermoelectric Effects

Three factors that effect thermoelectric devices are the Seebeck effect, the Peltier effect, and the Thomson effect.

1.1.1 Seebeck Effect

Due to the temperature difference between two different metals in the circuit, the voltage difference can be created (refer to Figure 1.1). This discovery was made in 1821, which belongs to physicist Tomas J. Seebeck [11]. The relation between the electrical voltage and temperature variation was correlated by the Seebeck coefficient, which is an inherent property of the circuit of two different metals [3, 6]. Potential difference can be given as:

$$V = \alpha \, \Delta T \qquad (1.1)$$

where V is electrical potential between two junctions of the circuit, α represents the Seebeck coefficient, and $\Delta T = T_h - T_c$ is temperature difference between junctions

(where, in the figure 1.1, T_h and T_c are hot and cold side temperature across the circuit, respectively). The symbol I indicates to the direction of the current applied in the circuit that is produced because of the voltage difference.

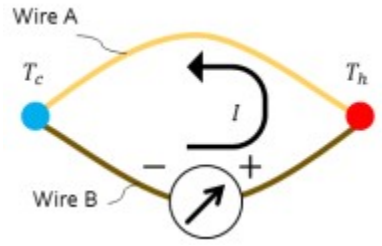

Figure 1.1 Seebeck Effect in the circuit of the two different metals [3].

1.1.2 Peltier Effect

In 1834, the French physicist, Jean Peltier, found that reverse of the Seebeck effect is correct also. When a potential difference was employed, heat was absorbed and released at the reverse sides in the same circuit of different metals [12]. The direction of heating or cooling in the circuit is determined by the direction of the current I. The relationship between the rate of heat transfer $Q_{Peltier}$ and current in the circuit was governed by the Peltier coefficient π that is written as:

$$Q_{Peltier} = \pi I \qquad (1.2)$$

The Peltier effect is illustrated in Figure 1.2 where the direction of heat rate into the circuit demonstrates the heat absorbed, and the direction of heat rate out of the circuit refers to heat released [3]. This also dictates the sign of the Peltier coefficient π makes a positive sign for the heat entering the system, while the heat that leaves the system dictates to be a negative sign. The Peltier effect is reversible between heat transfer and producing electricity; in another words, the influence either of generating heat rate from

electricity or resulting electric current from heat rate are interchangeable without a waste of energy [3].

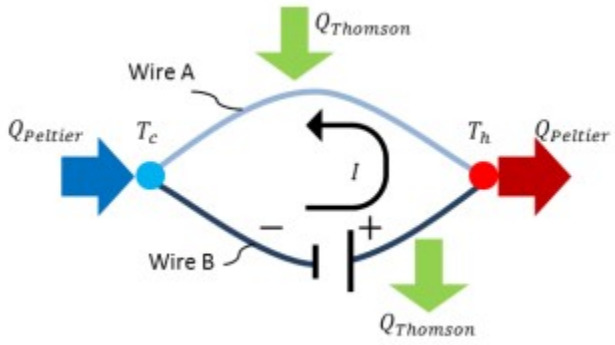

Figure 1.2 Peltier and Thomson Effect in a circuit of two different metals [3].

1.1.3 Thomson Effect

In 1851, William Thomson, who is later called Lord Kelvin, found that a following current with temperature gradient is either released or absorbed relying on the direction of current and material of conductor (see Figure 1.2).

$$Q_{Thomson} = \tau I \Delta T \qquad (1.3)$$

Equation (1.3) represents the relation between Thomson heat for both current flow I and temperature gradient ΔT, where τ is the Thomson coefficient. Identical to the Peltier effect, the sign is positive for heat absorbed (Wire A) and negative for heat released (Wire B). Furthermore, because the Thomson coefficient can be directly measured for individual materials, it is unparalleled, compared with the three thermoelectric coefficients [6].

All the three influences that are mentioned above give rise to the thermoelectric phenomena as a whole. These are not exclusive to thermoelectric materials alone but they

exist in all materials and semi-metals. These impacts are most often observable in different semi-metals (thermoelectric materials).

1.1.4 Figure of Merit and Thermoelectric Materials [3]

In order to measure the performance of particular TE devices, the figure of merit Z is utilized for this purpose, where it has units K^{-1}:

$$Z = \frac{\alpha^2}{\rho k} \qquad (1.4)$$

α represents the Seebeck coefficient with unit V/K, ρ represents the electrical resistivity of material with unit Ohm m, and k represents thermal conductivity of material with unit W/m K. There are two important ways to achieve a satisfactory value of the figure of merit Z (where a high value of figure of merit represents the great performance of cooling or heating). The first one is increasing the Seebeck coefficient α and reducing the electric resistivity of material ρ. In other words, a high power factor (α^2/ρ) is the first way to increase Z [3, 13]. The second method is decreasing the thermal conductivity of material. As it is known, thermal conductivity consists of a summation of two components, electronic and lattice thermal conductivity k_e and k_l, respectively, that can be given as ($k = k_e + k_l$). Both ρ and k_e are connected together by the Wiedemann-Franz law, which states that electronic thermal conductivity and resistivity rely on temperature.

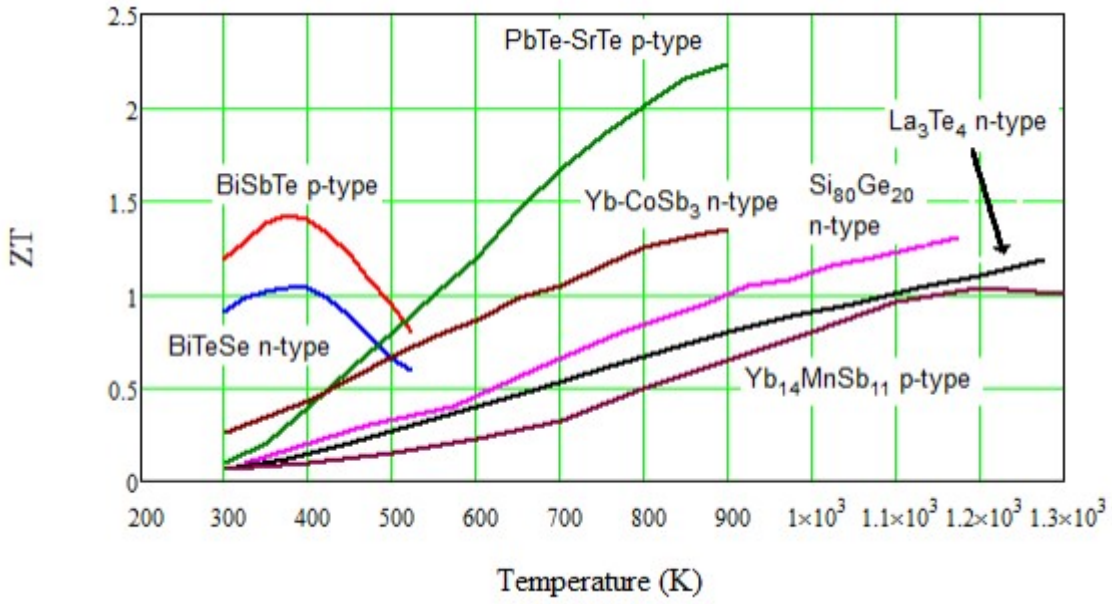

Figure 1.3 Dimensionless figure of merits for various nanocomposite thermoelectric materials [14].

Figure 1.3 illustrates dimensionless figure of merit *ZT* values of usually utilized TE materials. The highest value of *ZT* is represented by using bismuth telluride alloy ($Bi_2 Te_3$) for low to room temperature implementations. This characteristic makes bismuth telluride the preferable candidate for a plurality of cooling implementations as well as low-grade waste heat recovery. The current *ZT* value of bismuth telluride is commonly about 1.0 or a bit less. Nanostructures such as quantum wires have higher values of ZT around up to 1.4 [14, 15]. The implementations that have higher operating temperatures such as exhaust gas waste heat recovery commonly use materials that have a higher dimensionless figure of merit as a lead telluride (PbTe) compared to $Bi_2 Te_3$.

1.2 Miniature (micro) Thermoelectric Devices (μTE).

1.2.1 Background.

As explained in the instances presented previously, the concept of thermoelectric is developing in its uses and applications. Micro devices of the thermoelectric coolers with sufficient cooling potential, small size, and short response time are in high need in the telecommunication markets [16]. Not only μTECs, but also micro thermoelectric generators are utilized in many small low- power devices such as hearing aids or wristwatches. These miniature devices are widely used, such as medical applications, and microprocessor cooling [17].

The small size of thermoelectric generators has a large amount of the heat in a very small area that is also called the hot spot. Therefore, in recent years, many cooling methods for microprocessors were offered, such as air conditioners and refrigeration [18]. One of these techniques or methods is TEC, and is proposed to be a likely candidate with high dispersion capabilities and a miniature size. These miniature devices produce high cooling power density than these of traditional bulk material [19, 20].

However, minimizing thermoelectric devices size will create an important issue. This matter is represented by the losses that take place at the thermoelectric cooler or generator interfaces. These losses are indicated by electrical contact resistance and thermal resistance, which play a main role in the conventional bulk design. In addition, these losses become dominant when the element length of the thermoelectric is between 0.01- 0.06 mm and the losses effect thermoelectric performance [21, 22].

1.2.2 Current State in the Miniature Thermoelectric Devices

Many studies of miniature thermoelectric devices are explained in the literature, and are discussed in the literature review of this thesis. All the studies focus on minimizing size of the thermoelectric devices in order to obtain high cooling or heating power densities (cooling power per unit area of TE device) and high cooling performance. In other words, reducing the size of thermoelectric elements (take into account the electrical contact resistance and thermal resistance) has enabled the design to provide higher devices efficiency. Several of these studies are done either with experimental work or simulation work by using a method such as finite element analysis technique. In this research, the most helpful technique is presented to validate or predict most of the former and later studies.

This technique is an analytical approach that needs to be validated with experiments. Specifically, building and testing a miniature TE module is essential to confirm the accuracy of the analytical approach when compared to a realistic design.

CHAPTER II

2 THERMOELECTRIC BASIC (IDEAL) EQUATIONS

2.1.1 General Governing Equations

Before starting in illustrating theoretical design of miniature thermoelectric devices, the essential concept of thermoelectric should be discussed. Therefore, the primary objective of this chapter is to describe all related information about thermoelectric that help in understanding the related characteristics of the present study. This information is mostly utilized from Ref. [6] in addition to some adjustments.

In this part, the equations are in vector format to describe generalized three-dimensional cases. For material that has an isotropic substance, it is considered a non-uniformly heated thermoelectric material [3, 6]. So, the continuity equation for a constant current is written as:

$$\vec{\nabla}.\vec{J} = 0 \qquad (2.1)$$

The current density (or Ohm's law) and the temperature gradient (or the Seebeck effect) $\vec{\nabla}T$ have influenced on the electric field $\vec{E}$. Thus, electric field can be expressed by:

$$\vec{E} = \vec{J}\rho + \alpha\vec{\nabla}T \qquad (2.2)$$

The heat flux $\vec{q}$ can be written as:

$$\vec{q} = \alpha T\vec{J} - k\vec{\nabla}T \qquad (2.3)$$

where T is the temperature of the heat flux. The Peltier heat is indicated by the term $\alpha T\vec{J}$ and heat transfer is referred by the term $k\vec{\nabla}T$ that is given from Fourier's Law of conduction. The general heat distribution equation can be written as a function of the time:

$$-\vec{\nabla}.\vec{q} + \dot{q} = \rho_m c_p \frac{\partial T}{\partial t} \qquad (2.4)$$

where $\dot{q}$ represents the heat generated per unit volume, ρ_m represents the mass density of the material, c_p refers to the specific heat capacity and $\frac{\partial T}{\partial t}$ represents the rate of change of temperature with the time. When the steady state conditions are taken into consideration (time dependent), then the last term ($\partial T/\partial t$) in the equation (2.4) becomes zero. Equation (2.4) becomes:

$$\dot{q} = \vec{\nabla}.\vec{q} \qquad (2.5)$$

The electrical power is related with the rate of thermal energy in a relationship that can be written as:

$$\dot{q} = \vec{E}.\vec{J} = J^2\rho + \vec{J}.\alpha\vec{\nabla}T \qquad (2.6)$$

Insert equations (2.3) and (2.6) into equation (2.5)

$$\vec{\nabla}.\left(k\vec{\nabla}T\right) + J^2\rho - T\frac{d\alpha}{dT}\vec{J}.\vec{\nabla}T = 0 \qquad (2.7)$$

where $J^2\rho$ represents the Joule heating that exists in all current carrying materials, because of the interaction between electrical current and resistance, and the $T\frac{d\alpha}{dT}$ refers to the Thomson coefficient (τ) that was mentioned in Chapter I. There is almost good agreement between the exact solutions that take the Thomson effect into consideration and that ignore the Thomson effect ($\tau = 0$). This case was proved in some studies [23,

24]. Based on that, this research also supposes that the Thomson effect is neglected and that the Seebeck coefficient is independent of temperature.

2.1.2 Thermoelectric Couple Equations

The concept of a circuit of two different metals of a thermoelectric couple is defined as TE components that are connected to each other. These elements or components can be connected to either a load resistance (as in thermoelectric generators TEGs) or power supply (as in the thermoelectric coolers TECs). Each component can be described as a TE leg or a pellet. These elements can be either positively (indicated as p-types) or negatively (pointed as n-types) doped to modulate its thermoelectric properties [3].

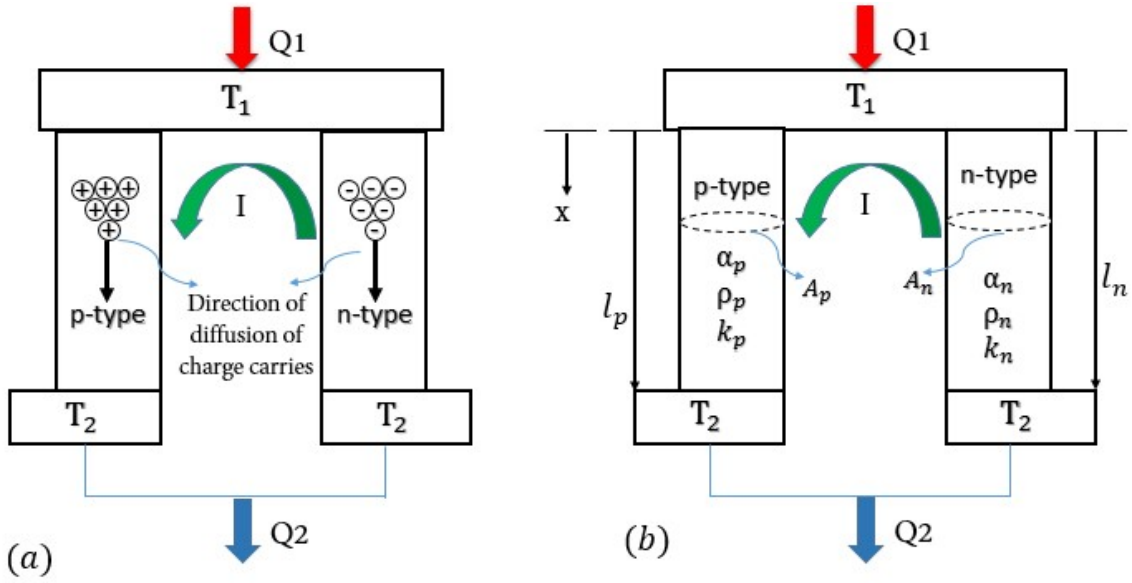

Figure 2.1 Longitudinal cross-section of a thermoelectric couple.

Both of these elements compose a TE couple and is utilized as the foundation to develop the governing equations of TE devices. Likewise, the charge carriers of the TE elements be more easily perturbed and freed when thermoelectric components are doped.

In the heating (power generation), there are free holes and electrons that are moving in the opposite directions because of the source of perturbation. Because of this movement, the direction of the current, within the thermoelectric couple, is with the holes' direction and the opposite direction is with electrons. Figure (2.1) (a) illustrates this movement. Therefore, the heat transfer occurs through carrying thermal energy by free electrons while traveling. The figure (2.1 b) represents a single thermoelectric couple that consists of two elements (p-type and n-type) with main material properties (Seebeck coefficient, thermal conductivity, and electrical resistivity) and geometric information such as element length (l_p,l_n) and cross-section area of element (A_p,A_n).

P-type and n-type components experience the same junction temperatures $T_1$and T_2 at opposite sides where uniform heat fluxes applies, and both elements are displayed to the same value of current I. The heat transfer rates that occur at junction temperatures (see Figure 2.1) are expressed as Q_1, and Q_2 respectively. The direction x (in Figure 2.2) is taken as a coordinate for reference of the system.

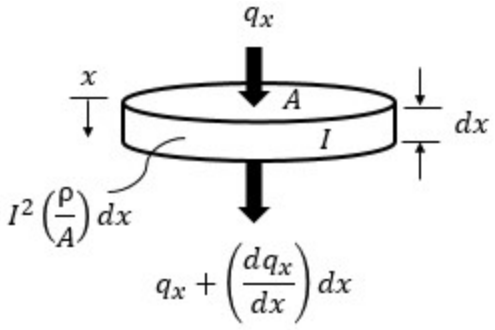

Figure 2.2 Differential element of a TE element.

Suppose a differential component of one of the TE elements with a cross-sectional area A of the element and differential length dx as illustrated in figure (2.2). A uniform

current that is applied to the differential element with electrical resistivity will cause Joule heating influences. The internal energy generated represented by Joule heating is supposed as the only source within the differential element [6]. The direction of the heat flow entry into the element assumes as a positive sign with supposing one-dimension case. Then, applying the energy balance to the differential element, the equation (2.5) becomes (where q_x refers to the heat flow)

$$q_x - \left(q_x + \frac{dq_x}{dx}\right)dx + \frac{I^2\rho}{A}dx = 0 \qquad (2.8)$$

Equation (2.3) multiplied by the area of the differential element becomes:

$$\vec{q} = \alpha T(x)\vec{J}_x - k\vec{\nabla}T \qquad (2.9)$$

where $\vec{J}_x = I\ /A$ and T(x) is function of direction x, so the equation becomes as:

$$\vec{q} = \alpha T(x)I - kA\frac{dT}{dx} \qquad (2.10)$$

At $x = 0$, plug it in equation (2.10):

$$\vec{q}_{x=0} = \alpha T(0)I - kA\frac{dT}{dx}\Big|_{x=0} \qquad (2.11)$$

By derivative equation (2.11) respect with direction x

$$\frac{dq_x}{dx} = -kA\frac{d}{dx}\left(\frac{dT}{dx}\right) \qquad (2.12)$$

Inserting equation (2.12) into equation (2.8) and rewrite it

$$q_x - \left(q_x - kA\frac{d}{dx}\left(\frac{dT}{dx}\right)\right)dx + \frac{I^2\rho}{A}dx = 0 \qquad (2.13)$$

Simplify equation (2.13) gives

$$kA\frac{d}{dx}\left(\frac{dT}{dx}\right) = -\frac{I^2\rho}{A} \tag{2.14}$$

Now, integrate equation (2.14) once time results

$$kA\int d\left(\frac{dT}{dx}\right) = -\frac{I^2\rho}{A}\int dx \rightarrow kA\frac{dT}{dx} = -\frac{I^2\rho}{A}x + C_1 \tag{2.15}$$

where C_1 indicates to a constant of integration. Again, limiting integration from $x = 0$ to $x = L$ for equation (2.15) and applying boundary conditions $(T\,(0) = T_1)$ and $(T\,(L) = T_2)$ give:

$$kA\int_{T_1}^{T_2}\frac{dT}{dx} = \int_0^L\left[-\frac{I^2\rho}{A}x + C_1\right] \rightarrow \quad kA\,[T(x)]_{T_1}^{T_2} = \left[-\frac{I^2\rho}{2A}x^2 + C_1x\right]_0^L \tag{2.16}$$

$$kA\,(T_2 - T_1) = -\frac{I^2\rho}{2A}L^2 + C_1L \tag{2.17}$$

Rearrange equation (2.17) expresses:

$$C_1 = \frac{kA\,(T_2 - T_1)}{L} + \frac{I^2\rho}{2A}L \tag{2.18}$$

Insert equation (2.18) into equation (2.15) at $x = 0$

$$\left.\frac{dT}{dx}\right|_{x=0} = \frac{(T_2 - T_1)}{L} + \frac{I^2\rho}{2kA^2}L \tag{2.19}$$

With same way at $x = L$ gives

$$\left.\frac{dT}{dx}\right|_{x=L} = \frac{(T_2 - T_1)}{L} - \frac{I^2\rho}{2kA^2}L \tag{2.20}$$

Substituting equation (2.19) into equation (2.10)

$$q_{x_{x=0}} = \alpha T_1 I - \frac{1}{2} I^2 \frac{\rho L}{A} + \frac{kA}{L}(T_1 - T_2) \qquad \textit{(2.21)}$$

Equation (2.21) indicates to both elements of the thermoelectric (p-type and n-type); it can be written for each element separated as

$$q_{x,p_{x=0}} = \alpha_p T_1 I - \frac{1}{2} I^2 \frac{\rho_p L_p}{A_p} + \frac{k_p A_p}{L_p}(T_1 - T_2) \qquad \textit{(2.22)}$$

$$q_{x,n_{x=0}} = -\alpha_n T_1 I - \frac{1}{2} I^2 \frac{\rho_n L_n}{A_n} + \frac{k_n A_n}{L_n}(T_1 - T_2) \qquad \textit{(2.23)}$$

As is known, the n-type element has a negative sign for the Seebeck coefficient because of being negatively doped. Therefore, to find the heat transfer for both p-and n-type at the direction $x = L$ and $T(x = L) = T_2$ can be given as:

$$q_{x,p_{x=L}} = \alpha_p T_2 I + \frac{1}{2} I^2 \frac{\rho_p L_p}{A_p} + \frac{k_p A_p}{L_p}(T_1 - T_2) \qquad \textit{(2.24)}$$

$$q_{x,n_{x=L}} = -\alpha_n T_2 I + \frac{1}{2} I^2 \frac{\rho_n L_n}{A_n} + \frac{k_n A_n}{L_n}(T_1 - T_2) \qquad \textit{(2.25)}$$

From Figure (2.1 b), seeing that $Q_1 = q_{x,p_{x=0}} + q_{x,n_{x=0}}$ and $Q_2 = q_{x,p_{x=L}} + q_{x,n_{x=L}}$. The heat rates of the TE couple at junction temperatures T_1 and T_2, respectively, are given as:

$$\mathrm{Q_1} = (\alpha_p - \alpha_n)\mathrm{T_1 I} - \frac{1}{2}\mathrm{I^2}\left(\frac{\rho_p \mathrm{L_p}}{\mathrm{A_p}} + \frac{\rho_n \mathrm{L_n}}{\mathrm{A_n}}\right) + \left(\frac{k_p \mathrm{A_p}}{\mathrm{L_p}} + \frac{k_n \mathrm{A_n}}{\mathrm{L_n}}\right)(\mathrm{T_1} - \mathrm{T_2}) \qquad \textit{(2.26)}$$

$$\mathrm{Q_2} = (\alpha_p - \alpha_n)\mathrm{T_2 I} + \frac{1}{2}\mathrm{I^2}\left(\frac{\rho_p \mathrm{L_p}}{\mathrm{A_p}} + \frac{\rho_n \mathrm{L_n}}{\mathrm{A_n}}\right) + \left(\frac{k_p \mathrm{A_p}}{\mathrm{L_p}} + \frac{k_n \mathrm{A_n}}{\mathrm{L_n}}\right)(\mathrm{T_1} - \mathrm{T_2}) \qquad \textit{(2.27)}$$

The following equations represent the relationship between the material properties of the p-type and n-type that can be given as:

$$\alpha = \alpha_p - \alpha_n \tag{2.28}$$

$$R = \frac{\rho L}{A} = \frac{\rho_p L_p}{A_p} + \frac{\rho_n L_n}{A_n} \tag{2.29}$$

$$K = \frac{kA}{L} = \frac{k_p A_p}{L_p} + \frac{k_n A_n}{L_n} \tag{2.30}$$

where R and K indicate to electric resistance and thermal conductance for both elements (p-type and n-type), respectively. Substituting equations (2.28) to (2.30) into equations (2.26) and (2.27) that gives:

$$Q_1 = \alpha T_1 I - \frac{1}{2} I^2 R + K(T_1 - T_2) \tag{2.31}$$

$$Q_2 = \alpha T_2 I + \frac{1}{2} I^2 R + K(T_1 - T_2) \tag{2.32}$$

Both equations (2.31) and (2.32) are called henceforward in this research as standard (ideal) equations. Regardless of the sign, the first expression in equations (2.31) and (2.32) αTI indicates to the Peltier/Seebeck effect and is reversible. The Seebeck coefficient considers the dominant force of the thermoelectric, the powerful Seebeck impact, the larger influence of heating, and cooling or power generation. The second idiom of two equations represents the Joule heating which is produced from interaction between the electrical current and resistance and works against the essential aim to cool or generate power [3]. The last expression represents the thermal conduction, which forms because of a temperature gradient in each material and works against the cooling

power of the thermoelectric coolers as well. Keep in mind that the Joule heating and conduction expression are irreversible.

2.1.3 Thermoelectric Modules

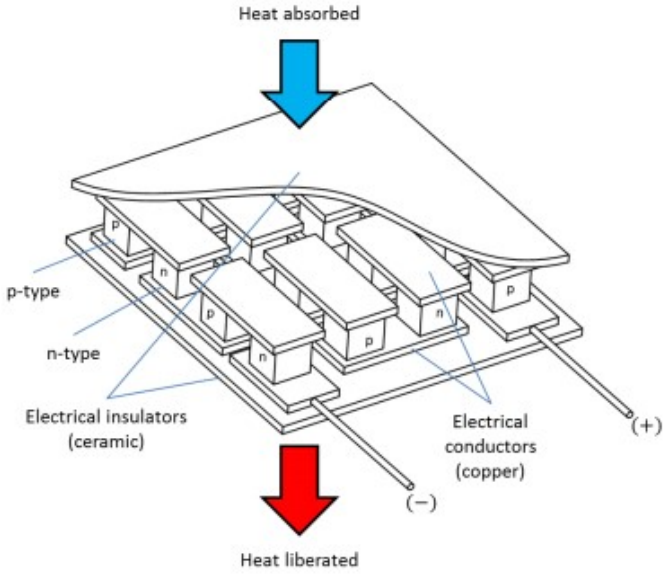

Figure 2.3 Cutaway of a thermoelectric cooler module [3].

The thermoelectric couple, which consists of p-type and n-type elements, represents the core structure of a thermoelectric device. These thermoelectric couples consequently are the basis for building a thermoelectric module. Figure 2.3 shows a conventional thermoelectric module, which forms of several TE couples attached to each other by electrical electrodes (conductors) and sandwiched between two ceramic plates. The thermoelectric elements are arranged with electrodes to connect the TE couples together electrically in series. The ceramic plates work as an insulator to not allow the electrical electrodes and TE couples from shorting while permitting the couples to be connected thermally in parallel [3, 6]. The upper part of each couple is subjected to a

similar constant temperature T_c while the lower part of each couple is at another constant temperature T_h in the thermoelectric coolers condition as is shown in Figure 2.4.

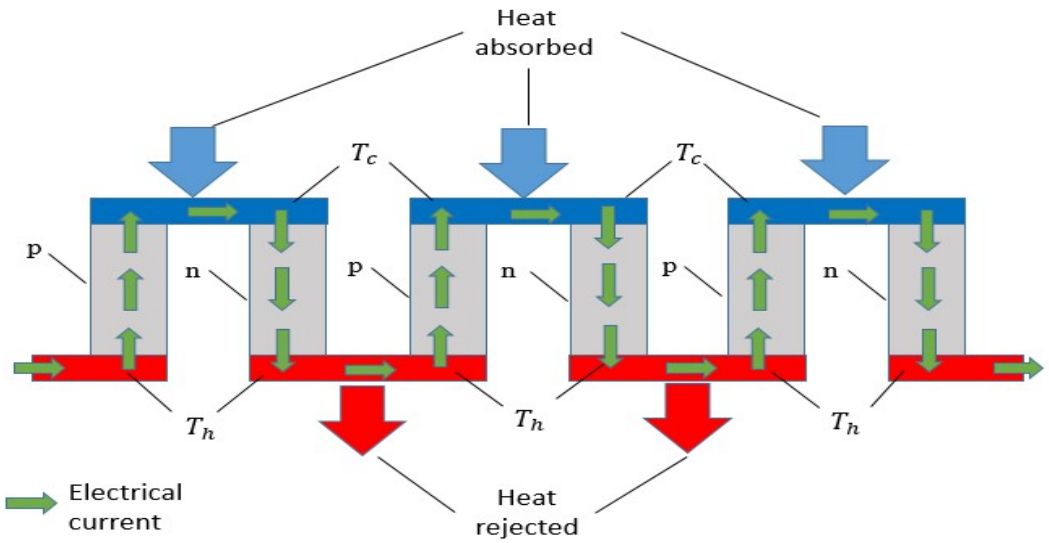

Figure 2.4 The electrical and thermal connectivity of TEC couples within a module.

2.1.4 Thermoelectric Generators (TEGs) Standard Equations

The task that thermoelectric generator devices do, is to convert temperature differences across TE devices, or to convert thermal energy immediately into useful electricity. The power output that is produced of TEG is connected to consuming devices that have an electrical load related with it as is illustrated in Figure 2.5. In equations (2.31) and (2.32), the junction temperatures T_1 and T_2 is replaced by T_h and T_c, respectively.

$$Q_h = \alpha T_h I - \frac{1}{2} I^2 R + K(T_h - T_c) \qquad (2.33)$$

$$Q_c = \alpha T_c I + \frac{1}{2} I^2 R + K(T_h - T_c) \qquad (2.34)$$

where Q_h and Q_c represent the heating and cooling power rates at hot and cold junction temperatures of the thermoelectric generator, respectively.

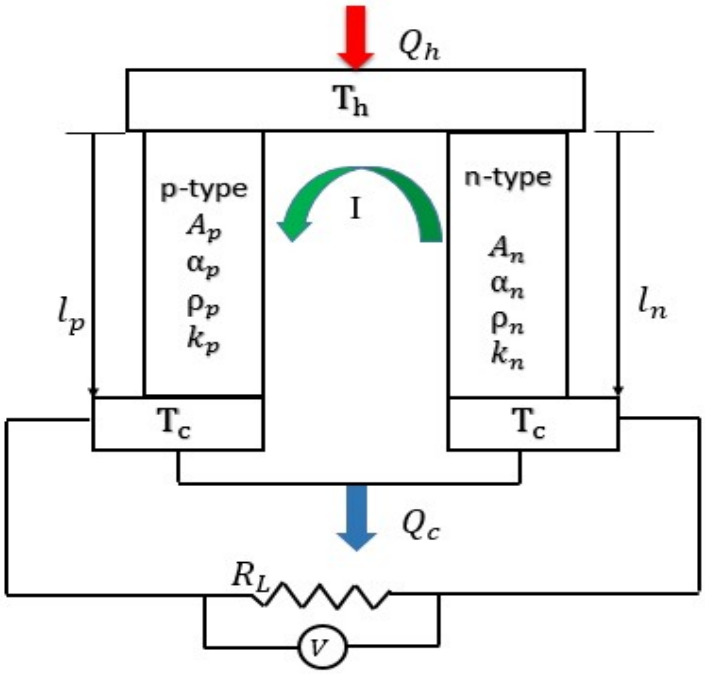

Figure 2.5 TEG connected to a load resistance.

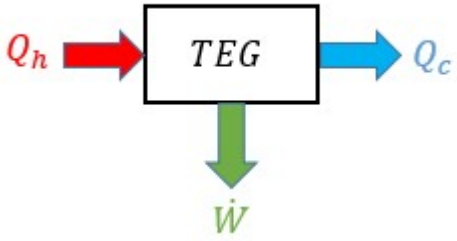

Figure 2.6 Energy balance for TEG.

Imagine that the TEG is similar to a heat engine of the first law of thermodynamics, which states that the sum of energies entering be equal to sum energies leaving. In the Figure 2.6, the sign for energy (heat flow) entering into the system is considered as a positive sign, while the powers that are leaving the system are considered

the negative sign. The difference between liberated and absorbed heat gives the power output as:

$$\dot{W} = Q_h - Q_c \tag{2.35}$$

$$\dot{W} = \alpha I(T_h - T_c) - I^2 R \tag{2.36}$$

In the same way, the power output could be calculated by utilizing load resistance (indicate to Figure 2.5) instead of internal resistance as:

$$\dot{W} = I^2 R_L = VI \tag{2.37}$$

Where V represents the voltage across the load resistor. From Ohm's Law also can calculate the voltage as:

$$V = IR_L = \alpha(T_h - T_c) - IR \tag{2.38}$$

From equation (2.37), $IR_L = \dot{W}/I$. The current can be computed from equation (2.38) as

$$I = \frac{\alpha(T_h - T_c)}{R_L + R} \tag{2.39}$$

The power output to input power ratio is called the conversion efficiency of the thermoelectric generator that can be written as:

$$\eta_t = \frac{\dot{W}}{Q_h} \tag{2.40}$$

Using equations (2.33) and (2.37) to give conversion efficiency in another term as:

$$\eta_{th} = \frac{I^2 R_L}{\alpha T_h I - \frac{1}{2} I^2 R + K(T_h - T_c)} \tag{2.41}$$

The main significant parameter for TEG in design is R_L/R (resistance ratio). From equations (1.4) and (2.39), the equation (2.41) is rewritten as

$$\eta_{th} = \frac{\frac{R_L}{R}\left(1 - \frac{T_c}{T_h}\right)}{\left(1 + \frac{R_L}{R}\right) - \frac{1}{2}\left(1 - \frac{T_c}{T_h}\right) + \frac{1}{2Z\bar{T}}\left(1 + \frac{R_L}{R}\right)^2 \left(1 + \frac{T_c}{T_h}\right)} \quad (2.42)$$

Where $\bar{T}$ represents the average temperature that is given as

$$\bar{T} = \frac{(T_h + T_c)}{2} \quad (2.43)$$

There are two ways of maximum parameters operation for a thermoelectric generator: maximum power efficiency or maximum conversion efficiency. The parameter that is variable in both these modes is the resistance ratio. However, the power output $\dot{W}$ in equation (2.36) can be differentiated with respect to the resistance ratio (R_L/R), and then set to zero [6].

$$\frac{d\dot{W}}{d\left(\frac{R_L}{R}\right)} = 0 \quad \Rightarrow \quad \frac{R_L}{R} = 1 \quad (2.44)$$

From equation (2.44)

$$R_L = R \quad (2.45)$$

Inserting equation (2.45) into equation (2.39) replaces the current to maximum powered current as:

$$I_{mp} = \frac{\alpha(T_h - T_c)}{2R} \quad (2.46)$$

From the same condition, equation (2.37) gives the maximum power as:

$$\dot{W}_{max} = \frac{\alpha^2(T_h - T_c)^2}{4R} \quad (2.47)$$

In addition, the maximum efficiency is written as:

$$\eta_{mp} = \frac{\left(1 - \left(\frac{T_c}{T_h}\right)\right)}{2 - \frac{1}{2}\left(1 - \frac{T_c}{T_h}\right) + \frac{4}{ZT_h}} \tag{2.48}$$

Alternatively, it can be written in Carnot efficiency terms (where $\eta_c = 1 - (T_c \,/\, T_h)$ as:

$$\eta_{mp} = \frac{\eta_c}{2 - \frac{\eta_c}{2} + \frac{4}{ZT_h}} \tag{2.49}$$

The other way of the maximum parameter operation is when the TEG runs at maximum conversion efficiency. Similar to power output, the thermal efficiency (Equation (2.42)) can be differentiated with respect to R_L/R then set it to zero,

$$\frac{d\eta_{th}}{d\left(\frac{R_L}{R}\right)} = 0 \quad \Rightarrow \quad \frac{R_L}{R} = \sqrt{1 + Z\bar{T}} \tag{2.50}$$

Where $\bar{T}$ indicates to the average junction temperature that can be given as:

$$\bar{T} = \frac{T_h + T_c}{2} = \frac{1}{2}\left[1 + \left(\frac{T_c}{T_h}\right)^{-1}\right] \tag{2.51}$$

According to this, the maximum current, power output, and efficiency becomes:

$$I_{mc} = \frac{\alpha(T_h - T_c)}{R\left(\sqrt{1 + Z\bar{T}} + 1\right)} \tag{2.52}$$

$$\dot{W}_{mc} = \frac{\alpha^2(T_h - T_c)^2\sqrt{1 + Z\bar{T}}}{\sqrt{1 + Z\bar{T}} + 1} \tag{2.53}$$

$$\eta_{max} = \left(1 - \frac{T_c}{T_h}\right)\frac{\sqrt{1 + Z\bar{T}} - 1}{\sqrt{1 + Z\bar{T}} + \frac{T_c}{T_h}} \tag{2.54}$$

2.1.5 Thermoelectric Coolers Standard Equations

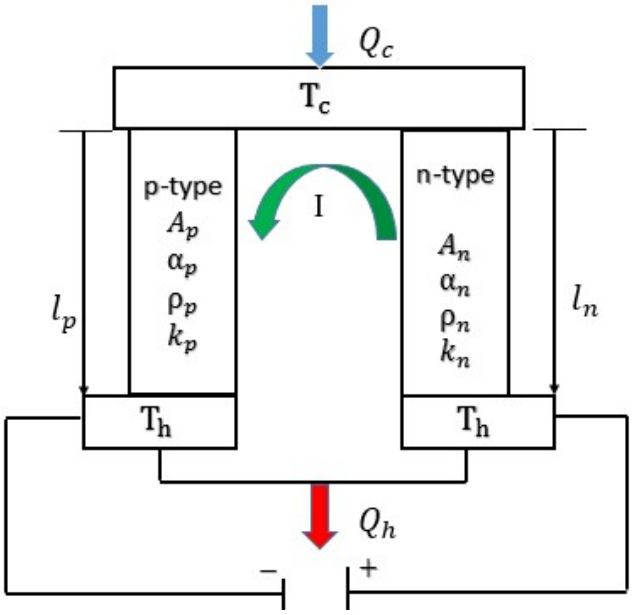

Figure 2.7 TEC connected to power supply.

Because the Peltier influence is reversible, delivering the current to a TE device leads to absorbed and release heat relying on the current flow. This impact becomes useful for essentially cooling and some heating applications [3, 6]. Equations (2.31) and (2.32) are written in terms cold and hot junction temperatures (T_c and T_h) instead of (T_1 and T_2), respectively.

$$Q_c = \alpha I T_c - \frac{1}{2} I^2 R - K(T_h - T_c) \qquad (2.55)$$

$$Q_h = \alpha I T_h + \frac{1}{2} I^2 R - K(T_h - T_c) \qquad (2.56)$$

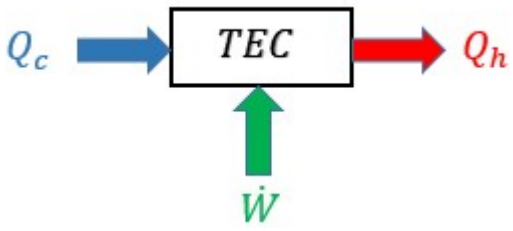

Figure 2.8 Energy balance for a TE cooler.

Employing the first law of thermodynamics to the system shown in Figure 2.8 to find the power output by TEC as:

$$\dot{W} = Q_h - Q_c \tag{2.57}$$

$$\dot{W} = \alpha I(T_h - T_c) + I^2R \tag{2.58}$$

The power used by thermoelectric cooler can be calculated from current I of the power apply and voltage V, resulting in:

$$\dot{W} = VI \tag{2.59}$$

From equations (2.58) and (2.59), the voltage V is written as:

$$V = \frac{\dot{W}}{I} = \alpha I(T_h - T_c) + IR \tag{2.60}$$

Interestingly, the voltages in equations (2.38) and (2.60) produced of TEG and TEC, respectively, are combination of both Seebeck and Ohm's Law voltages. The coefficient of performance COP, presented by heating (or cooling) power to the input power ratio, is a measure of performance of cooling devices:

$$COP = \frac{Q_c}{\dot{W}} = \frac{\alpha I T_{1c} - \frac{1}{2}I^2R - K(T_h - T_c)}{\alpha I(T_h - T_c) + I^2R} \tag{2.61}$$

The thermoelectric cooler has both modes of maximum cooling power and maximum coefficient of performance as in a thermoelectric generator, but the variable parameter in TEC is current applied. Equation (2.55) is differentiated with respect to the current supplied I and set it to zero and solve it for I to calculate the optimal current that is practically the maximum current for the presented material and geometry as [6]:

$$\frac{dQ_c}{dI} = \alpha T_c - IR = 0 \rightarrow I_{mp} = \frac{\alpha T_c}{R} \tag{2.62}$$

Applying the optimal (maximum) current, the maximum cooling power, voltage, and coefficient of performance can be computed by:

$$Q_{c,mp} = \frac{\alpha^2 T_c^2}{2R} - (T_h - T_c) \tag{2.63}$$

$$V_{mp} = \alpha T_h \tag{2.64}$$

$$COP_{mp} = \frac{\frac{T_c^2}{2} - \frac{(T_h - T_c)}{Z}}{T_c(T_c + 1)} \tag{2.65}$$

The maximum coefficient of performance can be calculated by differentiating equation (2.61) with respect to I and set it to zero as:

$$\frac{dCOP}{dI} = 0 \quad \Rightarrow \qquad I_{mc} = \frac{\alpha(T_h - T_c)}{R\left(\sqrt{1 + Z\bar{T}} - 1\right)} \tag{2.66}$$

Based on this maximum current:

$$Q_{c,mc} = \frac{\alpha^2 T_c(T_h - T_c)}{R\left(\sqrt{1 + Z\bar{T}} - 1\right)} - \frac{\alpha^2 (T_h - T_c)^2}{2R\left(\sqrt{1 + Z\bar{T}} - 1\right)} - K(T_h - T_c) \tag{2.67}$$

$$V_{mc} = \alpha(T_h - T_c)\left[1 + \frac{1}{\sqrt{1 + Z\bar{T}} - 1}\right] \tag{2.68}$$

$$COP_{max} = \frac{T_c}{T_h - T_c}\frac{\sqrt{1 + Z\bar{T}} - \frac{T_h}{T_c}}{\sqrt{1 + Z\bar{T}} - 1} \tag{2.69}$$

The maximum input current results the maximum cooling power at specific T_h and T_c, respectively. This gives the maximum current as:

$$I_{max} = \frac{\alpha T_c}{R} = \frac{\alpha\,(T_h - \Delta T_{max})}{R} \tag{2.70}$$

Where ΔT_{max} represents the maximum temperature difference at cold and hot junctions. The temperature difference (ΔT) is represented by:

$$\Delta T = T_h - T_c \tag{2.71}$$

When the current is at the maximum value, ΔT_{max} occurs with heat load at cold side equals zero ($Q_c = 0$), equation (2.55) is rewritten after current and temperature difference are replaced by maximum current and maximum temperature difference, respectively, as

$$\Delta T_{max} = \frac{\alpha^2 T_c^2}{2RK} = \frac{1}{2} Z T_c^2 \tag{2.72}$$

Equation (2.72) can be rearranged and written regarding hot junction temperatureT_h as:

$$\Delta T_{max} = \left(T_h + \frac{1}{Z}\right) - \sqrt{\left(T_h + \frac{1}{Z}\right)^2 - T_h^2} \tag{2.73}$$

Equations (2.72) and (2.73) give a simplification of maximum temperature difference in terms both of cold and hot junction temperatures T_c and T_h, respectively. Inserting equations (2.72) and (2.73) into equation (2.55) and rewrite it as:

$$Q_{c,mp} = K(\Delta T_{max} - \Delta T) \tag{2.74}$$

Equation (2.74) indicates the maximum cooling power for a specific material property and geometry that occurs when $\Delta T = 0$. At this condition, the maximum cooling power is

$$Q_{c,max} = K\Delta T_{max} \tag{2.75}$$

Both equations (2.74) and (2.75) represent maximum cooling power, but the first one is at certain temperature differences and the second is the absolute maximum cooling power.

The maximum voltage is found at a maximum current with no heat load, equations (2.70) and (2.73) are inserted into equation (2.60) to get it in terms of cold junction temperature or hot junction temperature as

$$V_{max} = \frac{\alpha^3 T_c^3}{2R} + \alpha T_c = \alpha(\Delta T_{max} + T_c) = \alpha T_h \tag{2.76}$$

2.2 Assumptions of the Thermoelectric Ideal Equations [3]

Due to the definition of equations indicated in the former part, it is of significance to highlight the suppositions that are established within these equations to avert from underestimation or overestimation of a TE performance. One of these assumptions is (temperature –independent materials properties) neglect the Thomson influence as described in equation (2.7). The Thomson effect has a very small impact on the performance of TE in both coolers and generators that were improved analytically [23] and experimentally [24]. In addition, it is supposed that the interfaces between the ceramic plates that sandwich the TE components and the electrical electrodes that link the couples together are ideal. Actually, because of flaws in fabrication and assembly, two types of the resistances exist between electrodes and the junctions of each thermoelectric

element, which are electrical contact resistance and thermal resistance. In Figure 2.9, k_c indicates thermal conductivity for both substrates and electrical electrodes, while ρ_c presents the electrical contact resistance between ceramic plates and conductors. Because of these two resistances, the cold and hot junction temperatures are T_{c1} and T_{c2}, and that differ from T_1 and T_2, respectively. Therefore, in this study, the electrical contact resistance and thermal resistance are included in standard (ideal) equations as assumption values, not as a measured value. These contacts become effective with reducing the element length of the thermoelectric module, therefore, the contact resistance is taken into account during the design in this research.

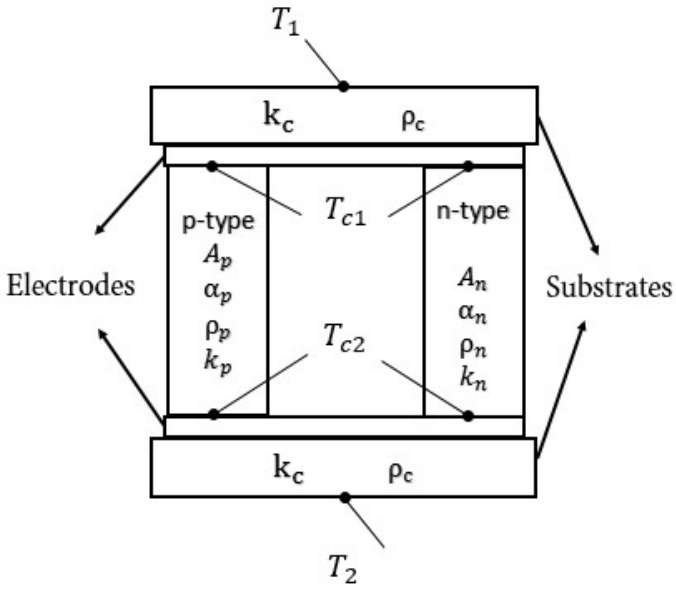

Figure 2.9 Configuration of thermoelectric couple considering contact resistances.

Furthermore, there are losses on all sides of the TE elements occurring through convection and radiation in the real operation. In manufacturing, the outer parts of the thermoelectric module are insulated to avoid convective losses. Similar losses are

supposed to be negligible in many cases including this research. In addition, the thermal resistance of the conductors is negligible [14].

2.3 Chapter Discussion

Most of the significant concepts that are required to understand the essential elements of thermoelectric from a thermal design perspective are discussed in this Chapter. These concepts are considered basic to studying and understanding the current study. Consequently, the literature of miniature thermoelectric system can be reviewed to find out the current situation and study if there is any room for further development.

CHAPTER III

3 OBJECTIVE AND LITERATURE REVIEW

3.1 Problem Statement and Objective

The state- of- art- of the technology method is discussed in this chapter to search about current study and specify its aim. The literature review part focuses on miniature thermoelectric devices and related studies that are required for the current research. During understanding the essential concept of thermoelectric, it is found that the effect of the contact resistance should be included into basic equations when small sizes of thermoelectric devices are used, because these resistances play a main role with reducing the TE size (reducing element length). Therefore, formulating a reliable technique that shows how contact resistance as well as the element length and ceramic substrates of the thermoelectric (studied in current research) play a significant role in the magnitude of the power density and performance of the thermoelectric devices. In addition, it is worth noting that all studies mentioned in the next section took into consideration contact resistance. Finally, studying of the miniature thermoelectric devices of the current work is investigated analytically. After the literature review is summarized, the main objective is shown in section 3.4.

3.2 Study of Previous Work

There are many studies on the miniature thermoelectric devices that are shown in literature. The first mention of the miniature thermoelectric device was presented by V. Semenyuk [21] in an international conference of thermoelectric in 2001, where a

theoretical and experimental work was made on miniature TEC module, which consist of seven modules of μTEC, to describe an available temperature lowering and maximum power density for short element of TE with different types of ceramic plates as is shown in Table 1. The results of the power density and maximum temperature difference were 80 W/cm^2 and 70 K, respectively, with element length 0.2 mm and ceramic plate type aluminum nitride AIN.

Table 1 Characteristics of Experimental 18-couple Samples (all dimensions are given in mm) [21]

Criteria	Modules with AIN substrate (k_c=180 W/m K)	Modules with AIN substrate (k_c=25 W/m K)
# of TE couples	18	18
Cross-section of TE elements	0.41*0.41	0.41*0.41
TE element length	0.2, 0.3, 0.53, 0.85, 1.05, 1.26, 1.6	
Ceramic plate area	4.2*4.2	4.8*4.8
Thickness of substrate	0.65	0.2 and 0.5

The module test was 1MC04-018 from Nord Company, Russia [21].

The same author, but in different study [22], made study to increase cooling power for miniature thermoelectric modules with thermo-element length 0.2 mm and 0.13 mm. The maximum power density at cold junction for a module that had an element 0.13 mm is about 110 W/cm^2 with ΔT=64 K. while the power density and maximum temperature difference were same to previous study.

Min and D. M. Rowe [25] made the theoretical model and validated experimentally on a single couple of a real thermoelectric generator, where the goal was to investigate the dependence of the electric power output on thermoelement geometry. The experimental work was applied on three commercial modules that have the same characteristics but with different element lengths. The results of testing these three modules confirmed that reducing thermo-element length by 55% increases power output by 48% with maintaining cold side at ambient temperature. In other words, reduction in thermoelement length from 2.54 mm to 0.5 mm leads to increasing in electric power about 75%.

The same author [26], but in different investigation, studied the effect of contact resistance on performance of TEG devices by measured the contact resistance experimentally. Their study showed the relation between contact resistance and thermo-element length and how it effects on performance of TE, where reducing the element length below 1.0 mm leads to decrease efficiency because of effect contact resistance. Figure 3.1 illustrates the relation contact resistance on conversion efficiency, where r indicates to contact resistance.

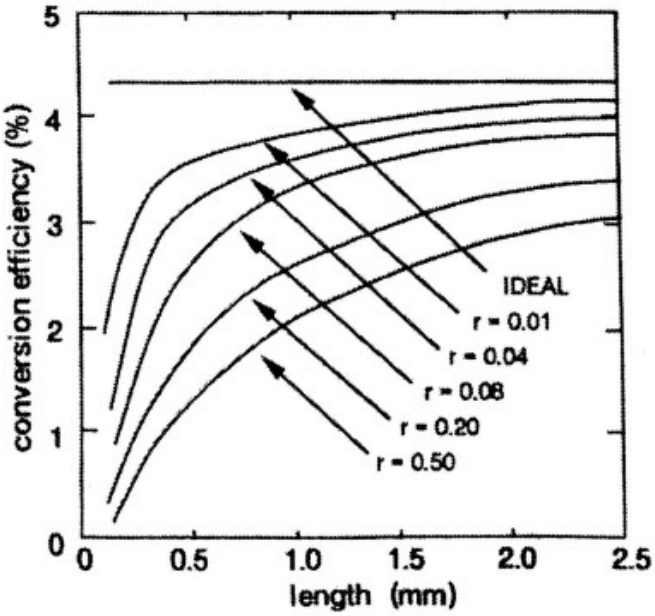

Figure 3.1 Conversion efficiency as a function of thermoelement length [26]

As it was mentioned in previous section, ceramic plates effect on cooling power (in case TECs) or power output (in case TEGs) and performance of thermoelectric devices. Semenyuk and Fleurial [27] discussed influencing of the substrate material on the cooling performance of the micro thermoelectric cooler. The research applied on a micromodule, which has a thermo-element length about 0.2 mm, and cross section area of element is 0.16 mm^2. The maximum temperature difference was 67 K (Figure 3.2 a) with diamond substrate and cooling power about 12 W at cold junction (Figure 3.2b).

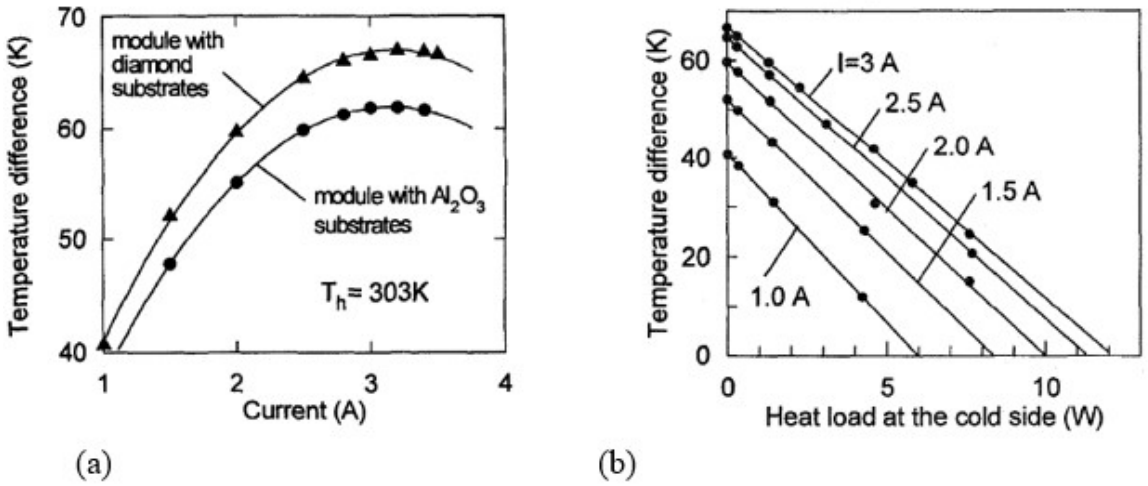

Figure 3.2 (a) Temperature difference dependence vs. input current, (b) Heat load characteristics of TE microcooler with diamond substrate (measured) [27].

Min and Rowe [28] made an analytical study to find an optimum length for the element of thermoelectric that lead to obtain on maximum cooling performance of an integrated thermoelectric microcooler (ITM). The result was that the optimum value of leg length was between 0.1-0.2 mm for ΔT_{max}, performance and Q_{max}.

On the other hand, some of the researchers depended on the simulation way that can show detailed solutions, which cannot be gotten through the experimental method and give information to guide in the design of μTECs devices [29]. W. Zhu and Y. Deng et al. [30] investigated the cooling power and cooling performance by using Finite Element Analysis Method (FEMs) to study the performance of micro thermoelectric coolers underneath various operating condition with various designs. The influences of the operating current, ratio of element length to cross section area of element, size, which considered as essential criteria in the proposed thermoelectric cooler modules, were considered into account. Their study showed the fact that minimizing size of TEC considers an adequate method to improve the cooling performance.

Optimizing the thermoelectric cooler geometry dimension is an alternate method to attain high cooling performance. Furthermore, formulate of a theoretical model and finite element method (FEM) to predict of the response of the thermoelectric devices is also fundamental to enhance the performance of these devices [29, 31].

Moreover, a numerical analysis of a micro-cooler was done by Pérez-Aparicio et al. [32] and Lee et al. [33] to study the impact of the thermoelectric and electrical properties of the material on the cooling performance. Kim et al. [34] and Wu et al. [35] investigated the influence of the thickness and the width-to-depth ratio on the performance of thermoelectric coolers. Chen et al. [36] also made a numerical study on the performance of thermoelectric coolers influenced by the Thomson effect. Goncalves et al. [37] made a theoritical study and FEM simulations where specifics of the fabrication method and initial results for the first on-chip thermoelectric micro-cooler mode, and ΔT of 15 K could be attained in each pixel.

3.3 Summary of Literature Review

Many designs of experimental and theoretical models have been improved in order to study the effect of contact resistance on module performance for miniature thermoelectric devices. Furthermore, element length and ceramic plates' effects on performance of modules have been studied as well. Some researchers have made a theoretical study and validated experimentally, and others have done numerical investigations and made comparisons with previous analytical or experimental work. Table 2 represents the summary of the literature review. Beneath the 'Results and Comparisons' column, only records with 'versus' (vs.) indicate cross-comparison, however, other entries indicate independent results.

Table 2 Summary of Literature Review

Author (s)	Module Type (s)	Results and Comparisons	Comments
V. Semenyuk	TEC	Theoretical vs. Experimental	Vacuum & miniature heater
Min and Rowe	TEG	Theoretical vs. Experimental	
V. Semeniouk et al.	TEC	Experimental	Diamond substrate
K. H. Lee et al. and	TEC	Simulation	
B. Jang et al.	TEG	Simulation	Three dimensional models
W. Zhu and Y. Deng et al.	TEC	Numerically	FEMs
Min and Rowe	TEC	Theoretical	ITM
Goncalves et al.	TEC	Theoretical vs. Simulation	
Kim et al.	TEC	Simulation	FEMs
J.L. Pérez–Aparicio et al.	TEC	Simulation	FEMs
Chen et al.	TEC		

3.4 Objective

After studying the essential concepts of thermoelectric devices, the aim of this research is to study the effect of contact resistance on the cooling power in the case of TECs and power output in the case of TEGs. Furthermore, the effect of thermoelectric dimensions, such as element length and substrates material (ceramic plates), is discussed deeply in this research, where the effect of contact resistance increases when the element length reduces below 0.5mm. Interestingly, the power increases with reducing thermo-element length until it reaches a maximum value at optimum element length of about 0.2 mm that is discussed in the next chapters.

Chapter IV discusses the main model and analytical modeling. The first section of the chapter studies the calculation of the material properties, and the modeling approach is discussed in a later part of the chapter. Chapter V shows how the experiment is set up to validate the modeling approach presented in Chapter IV. Finally, the analytical and experimental results were discussed in Chapter VI. This chapter also discusses the effective material properties for a commercial module and demonstrates the accuracy of the method that was developed by Lee et al. [38].

CHAPTER IV

4 MINIATURE THERMOELECTRIC MODELING

In this chapter, all information is in reference to the methodology shown and clarified in Ref. [21], and [22]. The goal of this chapter is to study the effect of contact resistance on minimizing thermoelectric devices and their performances. Figure 4.1 describes a single thermocouple of TE that has n- and p-type element sandwiched between the ceramic plates. The significant focus of the theoretical modeling is to develop a formula that helps in studying behavior the thermoelectric devices performances with considered impact electrical contact resistance and thermal resistance on μTECs and μTEGs by using thermoelectric ideal equations.

4.1.1 Calculating the Effective Material Properties

The effective material properties are explained here as the material properties that are calculated from the maximum parameters provided by the manufacturers (where maximum parameters are measured expermintally by manufactuaring) and are used instead of the intrinsic material properties because the manufacturing do not provide intrinsic material properties to consumers. The effective figure of merit is calculated from equation (2.73), which can be given as:

$$Z^* = \frac{2\Delta T_{max}}{(T_h - \Delta T_{max})^2} \tag{4.1}$$

In a similar way, the Seebeck coefficient can be found from equations (2.70) and (2.75) as:

$$\alpha^* = \frac{2Q_{c,max}}{I_{max}(T_h + \Delta T_{max})} \tag{4.2}$$

Also, effective electrical resistivity represents the next effective parameter by using equation (2.70):

$$\rho^* = \frac{\alpha^*(T_h - \Delta T_{max})A_e/l_e}{I_{max}} \tag{4.3}$$

The final effective parameter is effective thermal conductivity by using equation (1.4):

$$k^* = \frac{\alpha^{*2}}{\rho^* Z^*} \tag{4.4}$$

These effective material properties contain factual effects such as contact resistances [6]. Since the material properties are computed for a p-type and n-type thermoelectric couple, the material properties of a component (either p-type or n-type) can be gotten by dividing by 2.

4.2 Theoretical Analysis and Contact Resistance

It is known that the controlling factors additional to thermoelectric cooler miniaturization are represented by the values of the electrical contact resistance and thermal resistance, which sometimes increase the error between the realistic and theoretical equation models [6, 17]. They have different qualities, and various methods are employed to decrease them, where the electrical contact resistance is described mostly by the performance of the state-of-the-art method, while the smallest value of the thermal resistance relies on the thermal conductivity of available ceramic plates. The minimum possible value of electrical contact resistance is considered as ($1.6 * 10^{-6}$ Ω cm^2) [21], which is a suitable value in this research.

4.2.1 Realistic Formulas for Thermoelectric Generators. [6]

In this section, the formula of miniature thermoelectric generator is developed to study the effect contact resistance. The single thermocouple is taken from the thermoelectric module that has multiple thermocouples to investigate the influence of the contact resistances as shown in Figure 4.1.

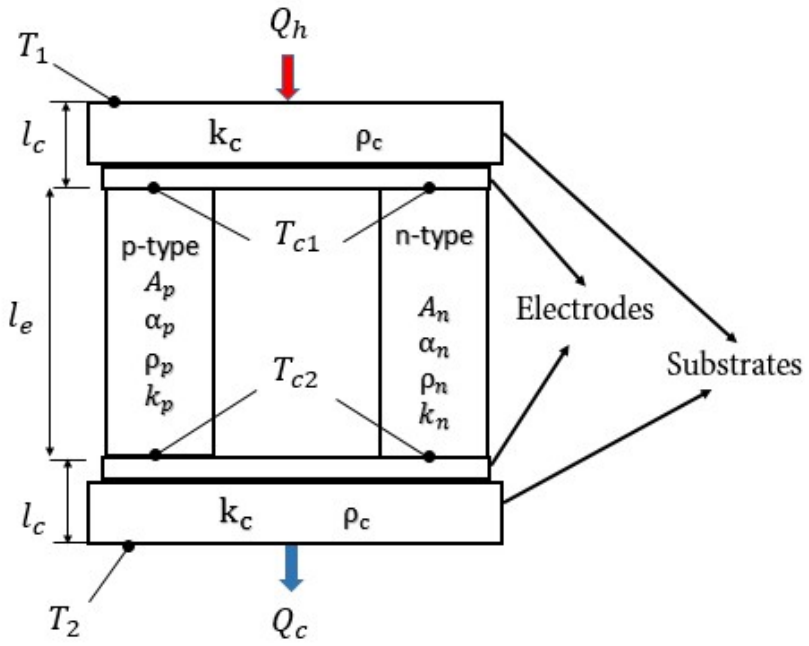

Figure 4.1 Basic configuration of a realistic thermoelectric couple, $T_1 > T_2$ [6].

At each side of thermocouple (upper and bottom), heat balance is given as (assume one thermocouple n-type and p-type only):

$$Q_c = \frac{A_e k_c}{l_c}(T_1 - T_{1c}) \tag{4.5}$$

$$Q_c = \alpha I T_{1c} - \frac{1}{2}I^2\left(\frac{\rho l}{A_e} + \frac{\rho_c}{A_e}\right) + \frac{A_e k}{l}(T_{1c} - T_{2c}) \tag{4.6}$$

$$Q_h = \alpha I T_{2c} + \frac{1}{2}I^2\left(\frac{\rho l}{A_e} + \frac{\rho_c}{A_e}\right) + \frac{A_e k}{l}(T_{1c} - T_{2c}) \tag{4.7}$$

$$Q_h = \frac{A_e k_c}{l_c} (T_{2c} - T_2) \tag{4.8}$$

$$I = \alpha \frac{(T_{1c} - T_{2c})}{R_L + \left(\frac{\rho l}{A_e} + \frac{\rho_c}{A_e}\right)} \tag{4.9}$$

where k_c indicates to the thermal conductivity which contain the thermal conductivity of substrates and the thermal contacts, l_e is element length of the thermocouple, l_c is thickness of both ceramic plates and conductors (contact layers), R_L is load resistance, and A_e is cross section area of element. The electrical resistance consists of two resistances: thermocouple and electrical contact [6] which is written as:

$$R = R_o + R_c = \frac{\rho l}{A_e} + \frac{\rho_c}{A_e} \tag{4.10}$$

Equation (4.10) is used in the calculation (as it shown in equations (4.6), (4.7), and (4.9)), or it can be simplified more as:

$$R = R_o + R_c = \frac{\rho l_e}{A_e}\left(1 + \frac{\rho_c}{\rho}\frac{1}{l_e}\right) = \frac{\rho l}{A_e}\left(1 + \frac{s}{l_e}\right) \tag{4.11}$$

So, the electrical resistance is written as:

$$R = R_o\left(1 + \frac{s}{l_e}\right) \tag{4.12}$$

where ρ represents the electrical resistivity that is given by $\rho = \rho_p - \rho_n$, s refers to the ratio of electrical contact resistivity to electrical resistivity of the thermoelectric module (ρ_c/ρ), and $R_o = \rho l_e / A_e$.

Equations from (4.5) to (4.9) are used numerically by using a mathematical program to calculate cold and hot junction temperatures (T_{1c} , and T_{2c}), respectively as a function of the load resistance R_L, cold side temperature T_1, cross section area of element

A_e, thickness of ceramic plates with conductors l_c, electrical contact resistance ρ_c, and thermal conductivity of the ceramic plates k_c, which deliver the heat flow rates Q_c and Q_h and the conversion efficiency η for a thermoelectric generator as:

$$T_{1c} = T_{1c}(R_L, T_1, A_e, l_c, \rho_c, k_c) \quad (4.13)$$

$$T_{2c} = T_{2c}(R_L, T_1, A_e, l_c, \rho_c, k_c) \quad (4.14)$$

4.2.2 Realistic Formulas for Thermoelectric Coolers. [6]

Suppose one thermocouple of TE module for TEC is used to investigate the impact of the thermal and electrical contact resistances as seen in Figure 4.2. The formula is developed for the real coefficient of performance and cooling power of thermoelectric cooler, which contain the thermal and electrical contact resistance. Heat balance at steady state can be written as:

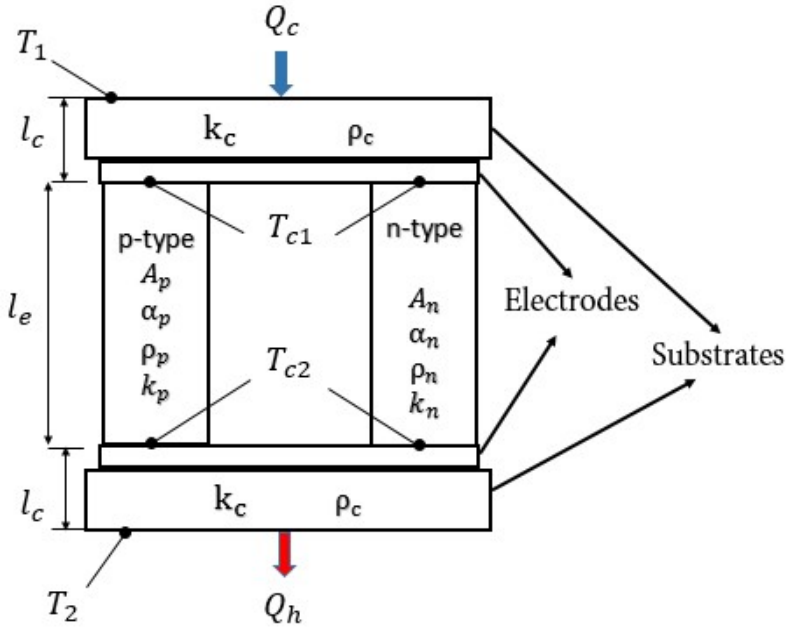

Figure 4.2 Basic configuration of a real thermoelectric couple, $T_1 < T_2$

$$Q_c = \frac{Ak_c}{l_c}\,(T_1 - T_{1c}) \tag{4.15}$$

$$Q_c = \alpha I T_{1c} - \frac{1}{2} I^2 \left(\frac{\rho l}{A} + \frac{\rho_c}{A}\right) - \frac{Ak}{l}\,(T_{2c} - T_{1c}) \tag{4.16}$$

$$Q_h = \alpha I T_{2c} + \frac{1}{2} I^2 \left(\frac{\rho l}{A} + \frac{\rho_c}{A}\right) - \frac{Ak}{l}\,(T_{2c} - T_{1c}) \tag{4.17}$$

$$Q_h = \frac{Ak_c}{l_c}\,(T_{2c} - T_2) \tag{4.18}$$

As for TEG, to calculate cold and hot junction temperatures, the four equations (4.15) to (4.18) was utilized and solved numerically by using a Mathcad program, as a function for current I, cross section area for component A_e, cold side temperature T_1, electrical contact resistance ρ_c, and thermal conductivity and thermal contact k_c, and leg length l_e, which can be given as:

$$T_{1c} = T_{1c}(I, T_1, A_e, l_c, \rho_c, k_c) \tag{4.19}$$

$$T_{2c} = T_{2c}(I, T_1, A_e, l_c, \rho_c, k_c) \tag{4.20}$$

It should also be noted Equations (4.5) to (4.9) and equations (4.15) to (4.18) represent one element of the thermocouple, it is multiplied by a number of element n to obtain the whole module.

4.3 Chapter discussion

Chapter IV discussed the theory that is required to understand the current work. Then, the formula that is needed to study the effect of the contact resistance was developed for both thermoelectric generator and cooler. This design was based on the analytical model that utilizes ideal equations including contact resistance of

thermoelectric system. In additional, the effective material properties were calculated and used instead of the intrinsic material properties.

CHAPTER V

5 EXPERIMENTAL STUDY OF MINIAATURE TE DEVOCES

This chapter illustrates the methodology explained in Ref. [21]. The purpose of this chapter is simply to explain the experimental setup that was built to study and validate the accuracy of the modeling design presented in Chapter IV. In the other words, the experimental results are used as a method to match the analytical (modeling) work. The aim is to explore how accurate the analytical is with the experimental part.

5.1 Experimental Description

When a thermoelectric module is operated as a cooling device, the main parameters that should be controlled to vary performance values are the junction temperatures (cold and hot) and current or voltage (input power to the device). Since all performances should be confirmed at steady state situations [3]. The temperatures must not be changed with time to ensure that the rate of heat transfer is at a clear value and is constant with time. Thermoelectric coolers mostly tested as cooling devices, but it can be used as heating when the polarity of a module is reversed. The current and DC voltage was delivered to the module by using a power supply. The cold side of the module is employed to the heat source. The most popular method is surface to surface solid heating using flat heaters [39] [40].

However, the heater is used in this study, consists of the cartridge heater inserted into aluminum block of high thermal conductivity. All the surfaces of the heater are

insulated except the one in contact with the TE module. A DC power source is applied to the heater to ensure continuous and constant power and attained the steady state situations. Since a TEC runs on the thermodynamic principle of a cooling power, the absorbed heat and input power must be released on its hot side.

While on the hot side, the forced fluid convection cooling is employed. Constant flow rate of this cooling fluid is very important to attaining and preservation steady state conditions. Secondary heat exchange processes are used to attaining liquid cooling where the absorbed heat from inside the fluid is rejected to the ambient by using a heat pumping or refrigeration process. Therefore, bath temperature controller is utilized to achieve such conditions. Recirculating bath temperature controller that is called Thermo Scientific NESLAB RTE 7 was used to maintain on hot side temperature.

5.1.1 Experimental Setup

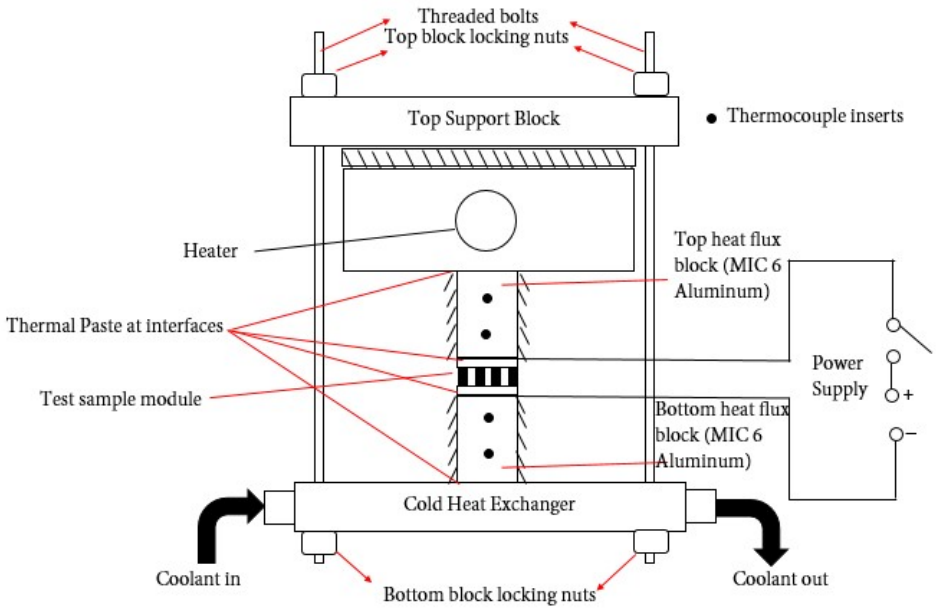

Figure 5.1 Schematic of experimental setup.

The setup employed in this research was designed to validate the theoretical analysis of the miniature TEC device. The test stand has enough place for commercial thermoelectric modules with areas of up to 40*40 mm^2, but the thermoelectric area used in this study is 3.81*3.81 mm^2. Figure 5.1 illustrates the setup of the test stand connected to a circuit that consists of a power supply while Figure 5.2 displays a schematic of the test stand with the side insulation pad removed.

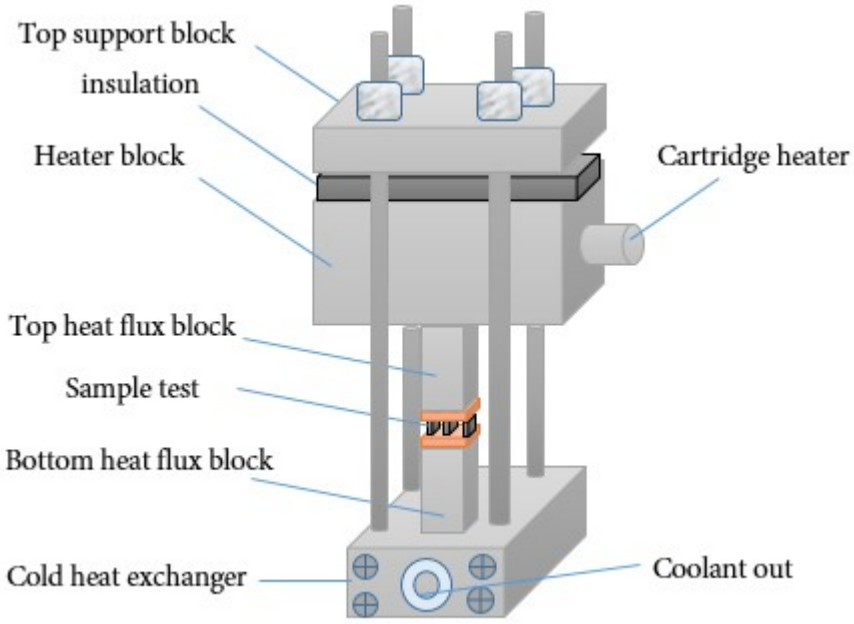

Figure 5.2 Schematic of test stand (with remove side insulation).

When testing TEC, the power supply was employed. The type of the power supply that applied to TEC was a TCR 10 20S30D-2-D model (see Figure 5.3) that has an output of up to 20 V of DC voltage and 30 A of DC current.

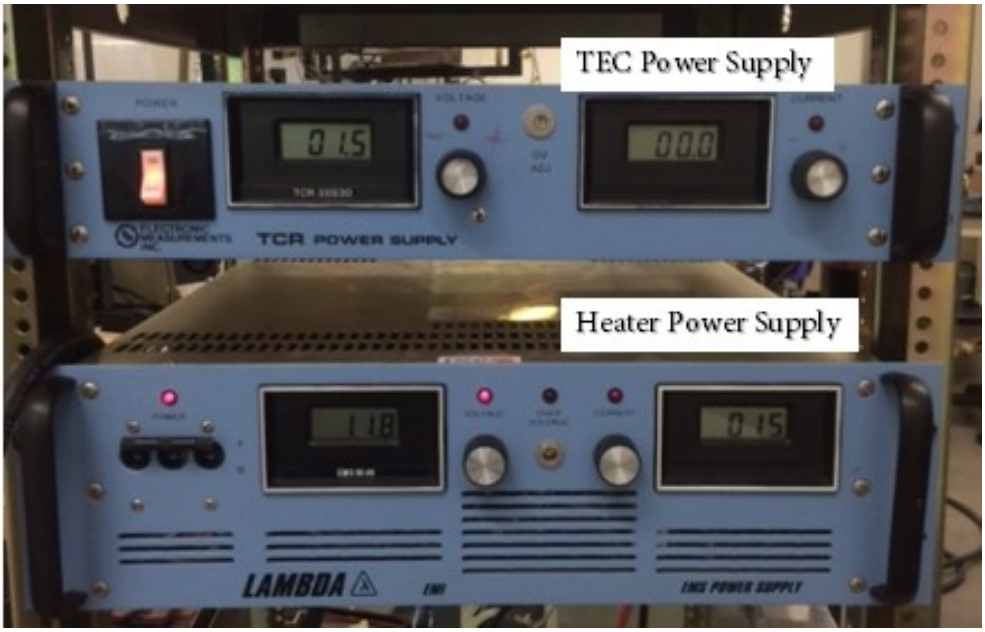

Figure 5.3 Power supplies (into heater and TE device).

The heat was provided by a heater block that is formed of one cartridge heater inserted within. The cylindrical cartridge heater was fabricated by Omega Engineering, Inc. (part no. CSS-403300/120V) and has dimensions of 15.875 mm (5/8") in diameter and 88.9 mm (3.5") in length. The cartridge was rated to have up to 7.75 W/cm^2 of power per unit area. The heater was applied by the power supply of TDK-Lambda EMS 80-60 model (Figure 5.3) with maximum power 5000 W (60 A of DC and 80 V).

The bath temperature controller is mentioned in the previous section, has capable to providing a temperature range between 248 K and 423 K. While the fluid utilized was glycerin/water 50/50 with freezing and boiling temperatures of 250.2 K and 379 K, respectively. An internal heater 0.8 kW was employed with a PID control to keep the recirculating liquid at a required operation temperature.

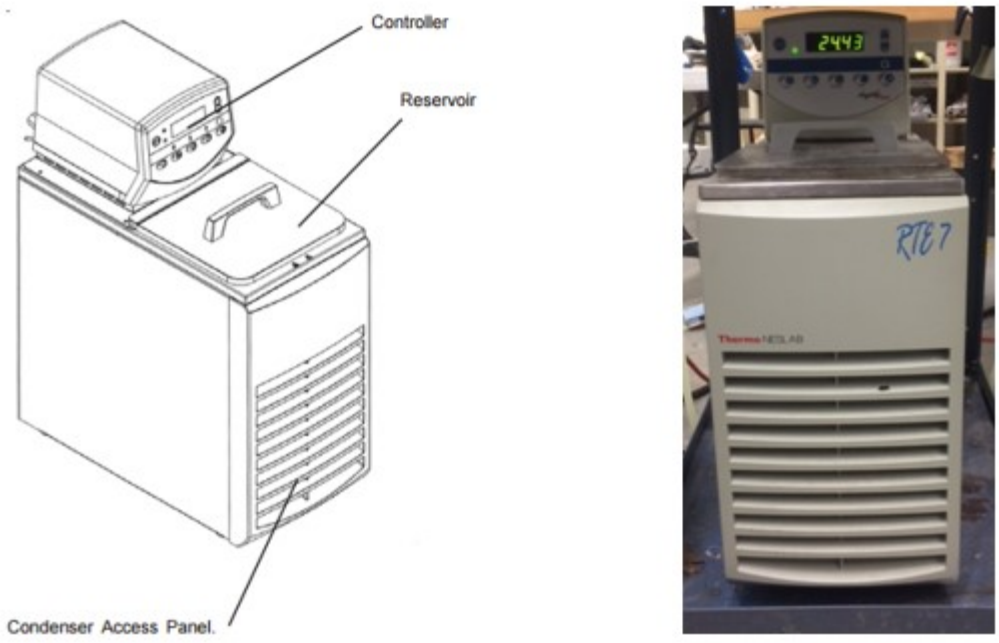

Figure 5.4 Test stand recirculating bath temperature controller.

The heater and cold side sources sandwiched the module with respective heat flux blocks in between. These blocks were fabricated from MIC 6 aluminum metal with an estimated thermal conductivity of 1.42 W/cm K [3]. Each aluminum block had dimensions (width, depth, and height) as 4 mm * 4 mm * 10 mm. Two thermocouples were inserted in each block in two slots on one vertical level with a perpendicular distance of 4.6 mm between each hole (center to center). A k-type thermocouple was used in standard stainless steel sheathing. Each slot had a diameter of 0.6 mm and a depth of 2 mm. The blocks' aluminum were insulated on all sides except the side that is connected to either a heat source or coolant with module's sides.

Table 3 shows the geometry properties (dimensions) of the test sample with effective material properties that were extruded from maximum parameters mentioned in previous sections. The cross section area of the thermoelectric element was measured by

using a microscope because the manufacturer does not provide these parameters to consumers. The type of microscope was a Nikon Measure scope as is illustrated in Figure 5.5.

Table 3 Characteristics of Experimental 18- couple Sample

Parameter (Symbol)	Unit (s)	Value (s)
Effect Seebeck Coefficient (α^*)	V/K	$2.151*10^{-4}$
Effect electrical resistivity (ρ^*)	Ω m	$8.097*10^{-6}$
Effect thermal conductivity (k^*)	W/m K	2.209
Cross section area of TE element (A_e)	mm^2	0.37*0.37
Element length (l_e)	mm	0.6
TE area (A)	mm^2	3.81*3.81
Number of TE element (n)	-	36
Substrate thickness (l_c)	mm	0.25

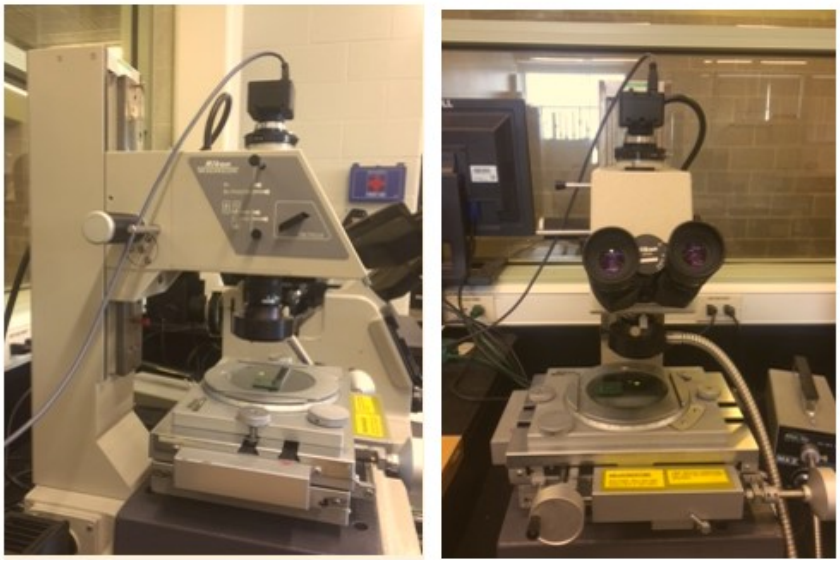

Figure 5.5 Microscope (Nikon Measure scope)

Due to the manufacturer provided dimensions of the test sample, such as width and long of the module, it was easy to measure it by microscope to create an equation that helps to convert pixel units to millimeter units because the microscope gives the dimension in pixel units, and it was hard to convert from pixel to millimeter directly (see Figure 5.6 a). After that, the element of the module was measured (Figure 5.6 b).

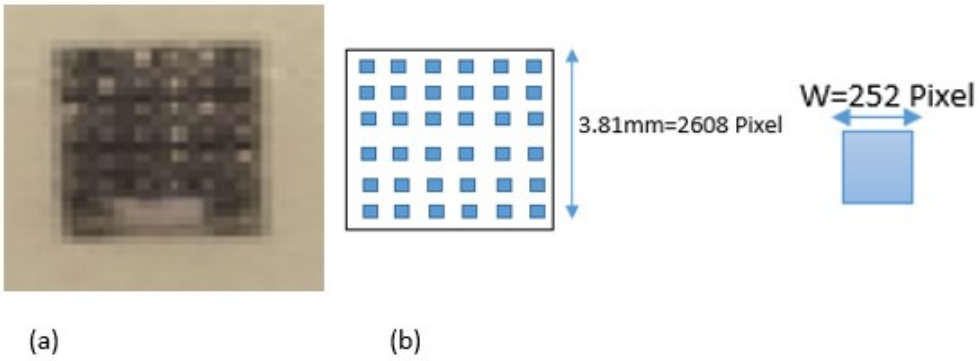

Figure 5.6 (a) Top view for real picture of module tested under microscope, (b) dimension explanation.

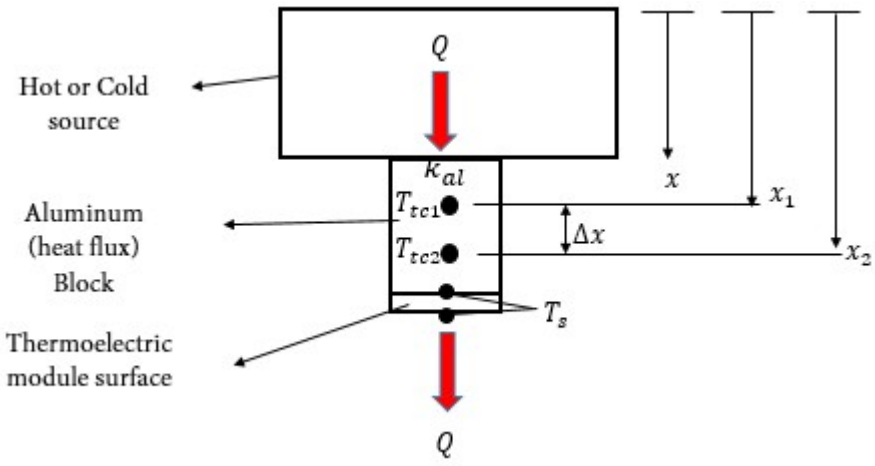

Figure 5.7 Temperature extrapolation and heat flux measurement.

These heat flux blocks had two objectives. The first was to measure the heat per unit area that takes place at the specific junctions of the module, and the second was to measure the cold and hot junction temperatures of the module through a linear process of extrapolation (see Figure 5.7), which illustrates the heat transfer diagram. With appropriate insulation and supposing excellent contact between interfaces as well as constant heat fluxes from the cooling or heating sources, the heat transfer rates need only to be taken into consideration one-dimensionally. The governing equation for the heat flux block for one-dimensional, steady-state conductive heat transfer, and no heat generation is written as:

$$\frac{d^2T}{dx^2} = 0 \tag{5.1}$$

Where T represents the temperature as a function of distance x. The boundary conditions are known (measured from thermocouple) can be given as:

$$T(x = x_1) = T_{tc1} \tag{5.2}$$

$$T(x = x_2) = T_{tc2} \tag{5.3}$$

By integration equation (5.1) two times respect with distance:

$$T(x) = Ax + B \tag{5.4}$$

The A and B are constant of the integration. At applying boundary conditions (equations (5.2) and (5.3)) gives a linear temperature distribution within the aluminum block that is

$$T(x) = \frac{T_{tc2} - T_{tc1}}{(x_2 - x_1)}x + T_{tc1} \tag{5.5}$$

Where $x_2 - x_1 = 4.6\,mm$, and T_{tc} and T_{tc2} are temperatures measured by thermocouples.

The major aim of employing the heat flux blocks was to make the process of the measurement of heat transfer rates accessible at the junctions of the module without having to account for losses that happened. Most prior study techniques used direct measurement of heat transfer rates from the heaters [41] or by using miniature heater [21]. The power provided to the heater was supposed to be the heat transfer rate received by the module. Appropriate insulation was used in order to decrease thermal losses that it considers a dull process. There are some effective techniques of insulating the heat source by utilizing guard heaters around the main heater to reduce the temperature difference between them, consequently eliminate as much conductive, convective and radiation losses [3].

The real heat flux into and out of the module can be directly calculated according to the provided thermocouple measurements. Employing Fourier's law of conduction and equation (5.5), the heat rate per unit area can be given as:

$$q'' = \frac{Q}{A_{al}} = -k_{al}\frac{dT(x)}{dx} = -k_{al}\frac{(T_{tc2} - T_{tc1})}{\Delta x} \qquad (5.6)$$

where A_{al} represents the cross section area of the aluminum block (or direction heat flux) and k_{al} refers to the thermal conductivity of the aluminum. The setup had thermal conductivity of aluminum 1.42 W/cm K [3] with cross section area 4*4 mm^2. The cold and hot sources from the heater and bath temperature controller were tested preliminary where they have shown consistent heat transfer throughout the aluminum block. This was indicated by the uniformity of temperature of any set of thermocouples; at steady state conditions, they differed no more than ±0.08 ºC. Furthermore, enough pressure was

employed between all interfaces sandwiching the module to decrease contact resistances utilizing threaded bolts and nuts.

5.1.2 Experimental Control

To make testing of TE module more precision at variation operating conditions, it needs to a certain degree of closed loop control. There are many manufacturers stipulate the baseline temperatures at which their products were tested. These values also sometimes become limitations factors to which the modules should be operated within. For thermoelectric coolers, the limiting factors to attain required performance are represented by hot side temperature. Closed loop control was used onto the test stand by handling the heater and bath temperature controller to control the junction temperatures at desired values.

Figure 5.8 illustrates the connection of two power supplies (one of the power supplies to controlling heater and other applying power to sample test) and thermocouples. Both power supplies and thermocouples were attached to a National Instruments data acquisition system (DAQ) that consists of an SCXI-1000 chassis with the SCXI-1303 isothermal terminal block. The thermocouples were connected to the terminal block that has a high-accuracy thermistor cold-junction temperature sensor permitting for a built-in cold junction reference when taking temperature measurements.

The power supply applied to the heat source had remote control ability and was attached to the DAQ through a PCI 6063-E analog terminal block. The data acquisition system was attached to PC while bath temperature-controller was connected directly to the computer utilizing RS 232 serial cable (see Figure 5.8).

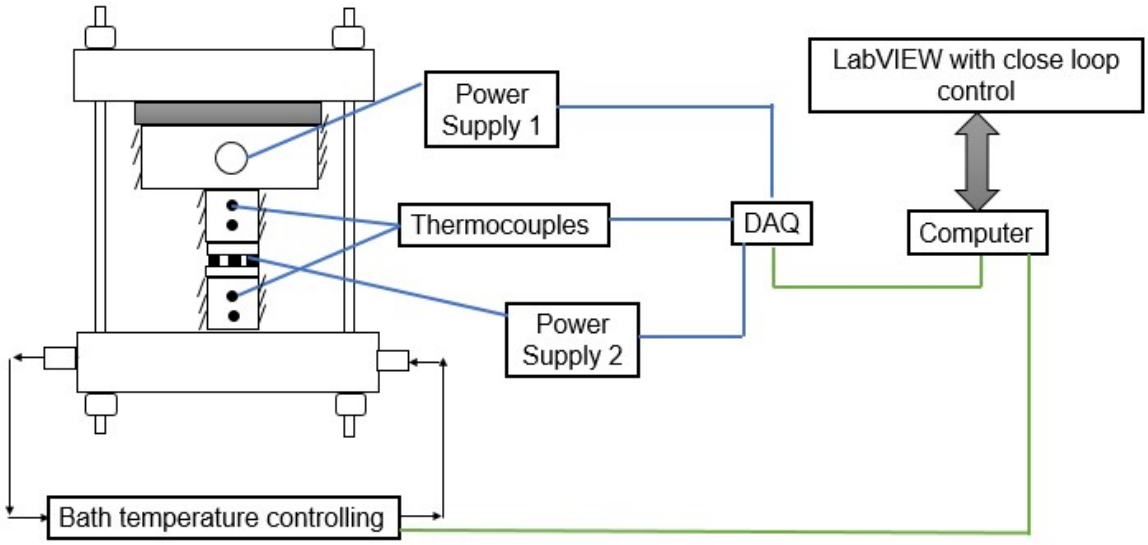

Figure 5.8 Overview of experimental control.

The temperature readings have sampling rate of 1 HZ or 1000 sample per second. Because the transient data was not essential to this experiment, the sampling rate set to 1 HZ or 1 sample per second. All data acquisition and equipment manipulation were attained utilizing National Instruments LabVIEW software to control the junction temperatures of the module. A Virtual Instrument (VI) was built in LabVIEW software, where VI integrated the power supplies, bath temperature controller, and as well as temperature readings from the thermocouples.

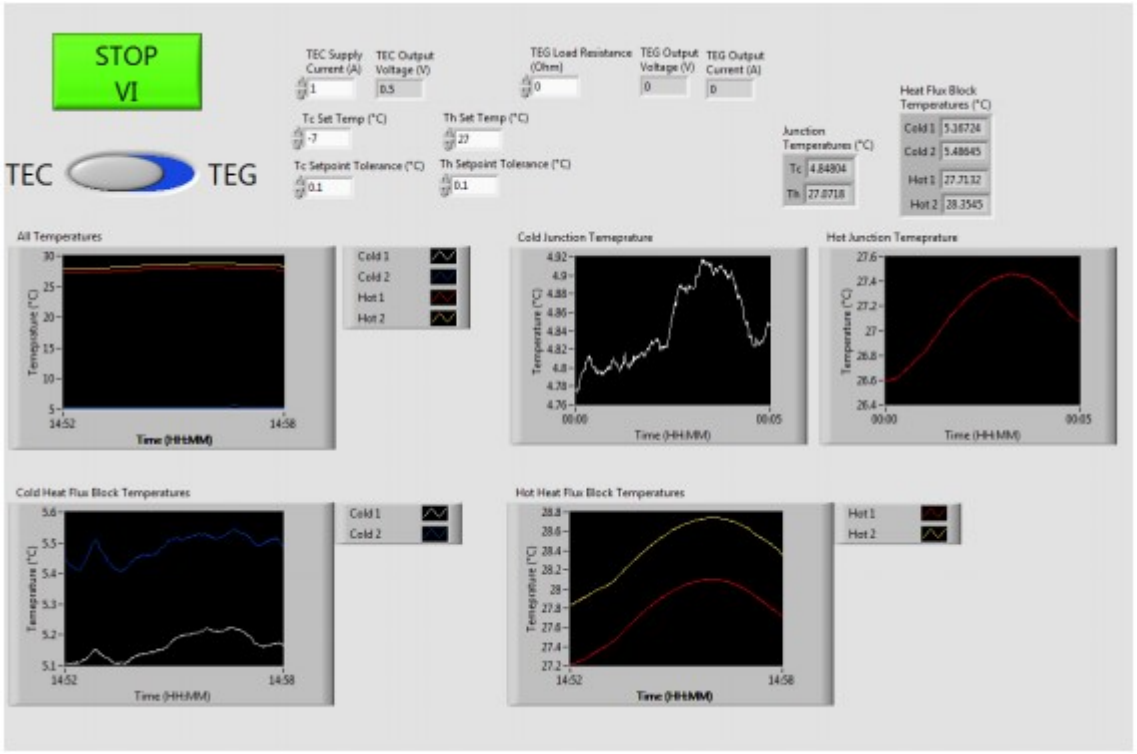

Figure 5.9 Front panel of data acquisition VI [3].

Figure 5.9 illustrates the front panel of the data acquisition VI. Four waveform graphs are showing the various thermocouple readings versus time. Two of them represent the junction temperatures of the test sample extrapolated from the thermocouple readings. Interestingly, the VI was achieved while the testing was still in the transient state.

5.1.3 Experimental Procedure

This section is a description of the proceedings required to obtaining performance data of a test sample. Figure 5.10 represents the means to get different data points that would be recorded or plotted to validate the performance of the specific module. The primary step in the program was to install the particular test subject between the aluminum blocks (heat flux) (see Figure 5.1). Due to micro cracks and surface defects on

the aluminum blocks, the extremely conductive thermal paste was employed onto such area to reduce thermal contact resistances. The uniform pressure was employed on the test system by utilizing bolts and nuts to assure perfect contact between the surfaces.

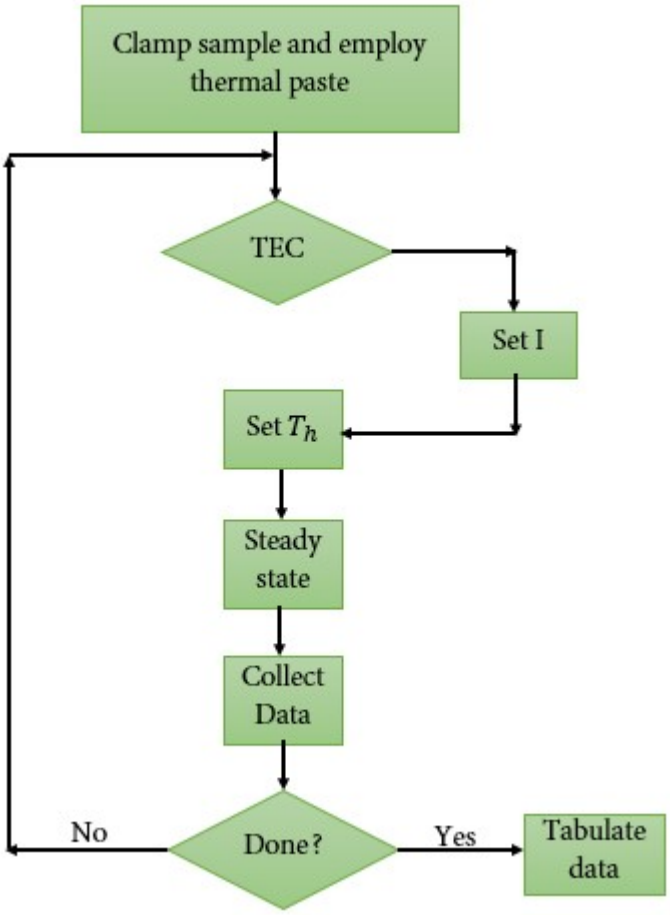

Figure 5.10 Flowchart of experimental performance evaluation.

The VI was executed and the test sample of a thermoelectric cooler was made. In the TEC measurement method, the power supply was connected to the module. When TEC was tested, then the needed current value was provided, or voltage could be provided instead.

The subsequent step was to specify the junction temperatures to which the bath temperature-controller would keep the test sample while it produced cooling. The monitoring system needed between 30 to 50 minutes to attain steady state situation. The waiting time will take the longer time with the increasing input power or higher different temperature across the module. Steady state situation was estimated by investigating a waveform chart that illustrates the temperature readings against time. The steady state should be attained when the temperature value stays stable for about 2-3 minutes. Then, the data can be collected into a spreadsheet file through VI.

CHAPTER VI

6 RESULTS AND ANALYSIS

Chapter VI begins with addreasing the results of the effective material properties for commorcial module. Then, an existing study of miniature thermoelectric devices, found in previous studies, was validated by utilizing the present model. Next, discusing the results of the present study for both miniature thermoelectric coolers and generators devices and compare it with large sizes. Finally, expermintal results are addressed in the last section of this chapter.

6.1 Effictive Material Properties

Consider a commercial miniature thermoelectric cooler module (SP5612-01AC) and from the provided manufacturer data sheet, the maximum parameters ($Q_{max}, I_{max}, V_{max}$, and ΔT_{max}) are obtained experimentally. Using maximum parameters and equations from (4.1) to (4.4) to calculate effective material properties. The performance curves for commercial module (μTEC) were evaluated analytically by applying the equation (2.55) with variation values of cooling power using effective materials properties. The geometrical information of the thermoelectric elements were measured, such as the number of elements n, cross-sectional area of the TE element A_e, and thermoelectric element length by using the microscope type "Nikon measure scope (see Table 3)". The process of obtaining these values meant that the module had to be irreversibly broken up, rendering them irreparable and non-functional. The effective material properties–were calculated for one element assuming the similar materials and

geometry between each TE elements. As previously mentioned, three out of four maximum parameters need to satisfy the effective material properties, which are calculated by using $\Delta T_{max}, I_{max}, and\ Q_{max}$.

Table 4 Effective Material Properties for SP5612-01AC

Criterion	Symbols (unit)	Value at $\boldsymbol{T_h = 27}$ ºC
Provided maximum Parameters	$Q_{max}\ (W)$	2.0
	$V_{max}\ (V)$	2.17
	$I_{max}\ (A)$	1.4
	$\Delta T_{max}\ (K)$	69
	$R_M\ (\Omega)$	1.32
Effective material Properties	$\alpha^*(\mu V k^{-1})$	215.082
	$\rho^*(\Omega cm^{-1})$.	$8.097*10^{-4}$
	$k^*(Wm^{-1}K^{-1})$	2.2
Effective maximum parameters	$Q_{max}\ (W)$	2.0
	$V_{max}\ (V)$	2.323
	$I_{max}\ (A)$	1.4
	$\Delta T_{max}\ (K)$	69
Effective figure of Merit	Z^*T_h	0.776

Geometric information: number of elements n=36, Cross-section area of TE element A_e=0.137 mm^2, element length of TE =0.6 mm.

Table 4 summarizes the effective material properties calculated for the SP5612-01AC μTEC module utilizing maximum parameters. When calculating the maximum effective parameters, predicted the Q_{max}, ΔT_{max}, $and\ I_{max}$ values exactly, while there is an error about 7% between predicted V_{max} values and the actual provided one. Figure 6.1, compares the original format of the commercial data points with the prediction from the model utilizing effictive material properties for temperature differences against current at constant cooling powers. The results were plotted by inserting cooling power (Q_c) to the required value in equation (2.55) and solving for ΔT as a function of current I . The prediction was agreed well to the data provided by manufacturer (see Appandix C).

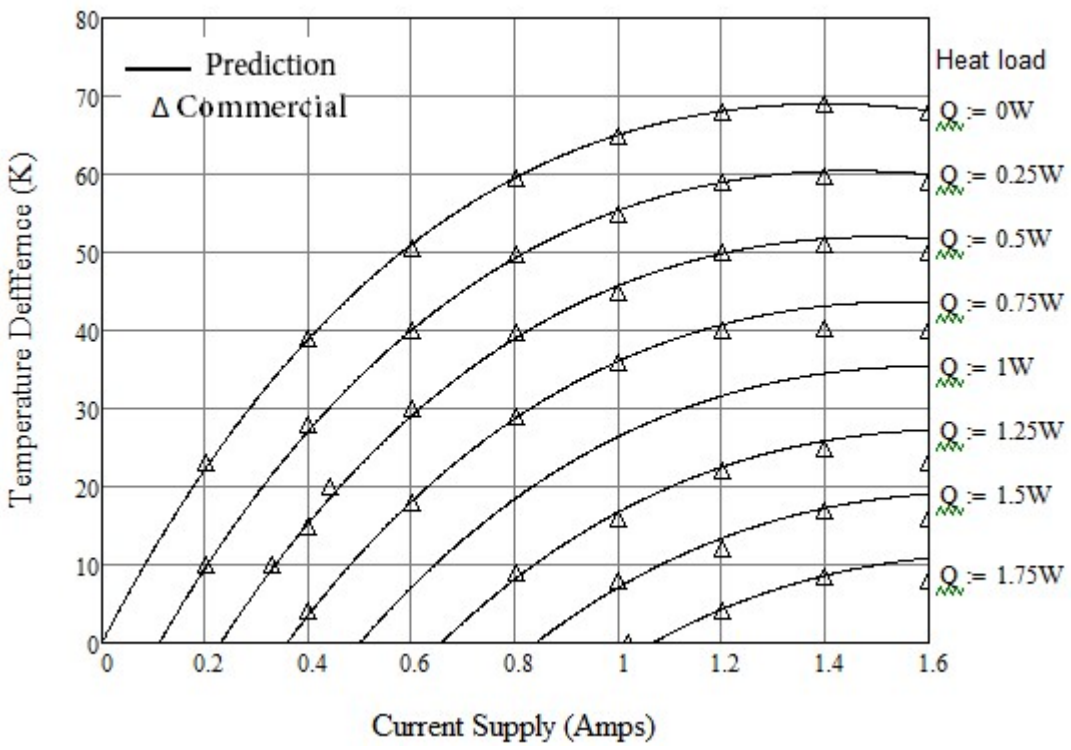

Figure 6.1 Analytical prediction vs. commercial data temperature difference comparison (at various cooling power) for SP5612-01AC.

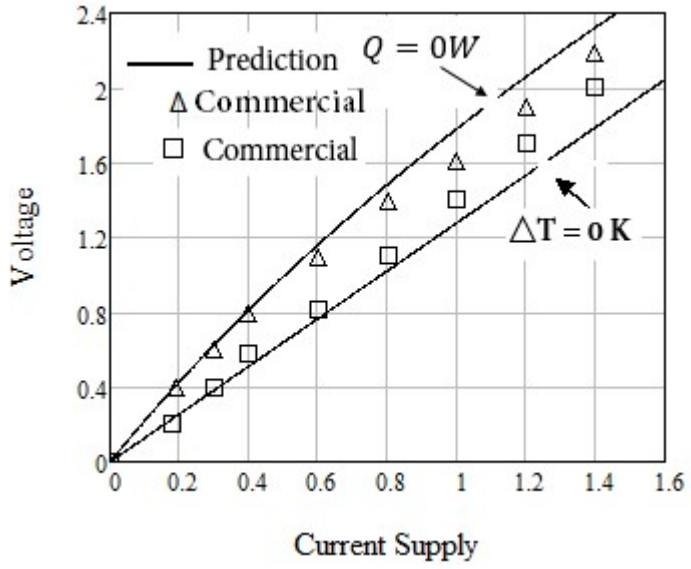

Figure 6.2 Analytical vs. commercial data voltage comparison for ASP5612-01AC.

The manufactures did not provide overall voltage versus current data other than only at two specific operating conditions: at setting cooling power to zero and temperature difference to zero. The first condition was satisfied by placing $Q_c = 0$ in equation (2.55) and solve it for ΔT as a function of current I. Both temperature difference and current were substitute into equation (2.60) to get the voltage V as a function of current when Q_c is zero. While at ΔT = 0, the voltage was taken directly from the equation (2.60). Figure 6.2 compares the analytical voltages with the commercial data and indicates a degree of discrepancy for the $Q_c = 0$ condition at increasing current values. It is important to mention that the voltage under $Q_c = 0$ condition shows a non-linearity because of the non-linear relation between temperature difference and current in equation (2.55).

6.2 Verification of Present Model

In this section, the experimental data provided by Semenyuk was re-produced using present model based on the input parameters provided by Semenyuk (referred to Table 5) and a real miniature thermoelectric cooler module is illustrated in Figure 6.3.

Table 5 Parameters for a Thermoelectric Cooler Module (IMC04-018-02) [21]

Criterion (Symbol)	Values (Unites)	Criterion	Values (Unites)
Seebeck Coefficient (α)	205 (μV/K)	T_2	303 (K)
Electrical Resistivity (ρ)		I_{max}	4.0 (Amps)
Thermal Conductivity (k)	1.4 (W/mK)	ΔT_{max}	70.0 (K)
Figure of merit (ZT) at 27 ºC	0.9		
Number of couples (n)	18		
Cross section area of TE element (A_e)	0.168 (mm^2)		
TE element high (l_e)	200 (μm)		
Substrate Area	4.2*4.2 (mm^2)		
Substrate thickness (l_c)	0.635 (mm)		
Substrate AIN thermal conductivity (k_c)	180 (W/mK)		
Electrical contact resistivity (ρ_c)	$1.6*10^{-6}$ (Ω cm^2)		

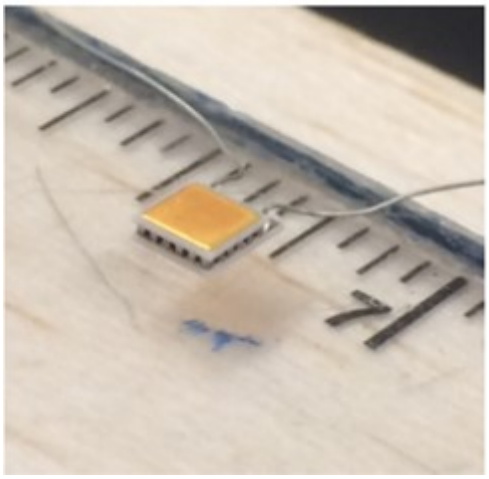

Figure 6.3 Miniature thermoelectric cooler module.

The maximum temperature difference was calculated by utilizing the current model developed. Which is obtained at adiabatic heat load, i.e. the cooling power is zero. Figure 6.4 compares analytical maximum temperature difference with experimental data and shows a good agreement. The characteristics of the graph shows a linear relationship from 0.5 to 2mm (max temp difference and length), but plunges down sharply below 0.5 mm value. This steep seems mostly because of the high temperature value at hot junction of TEC compared to the one at the heat sink.

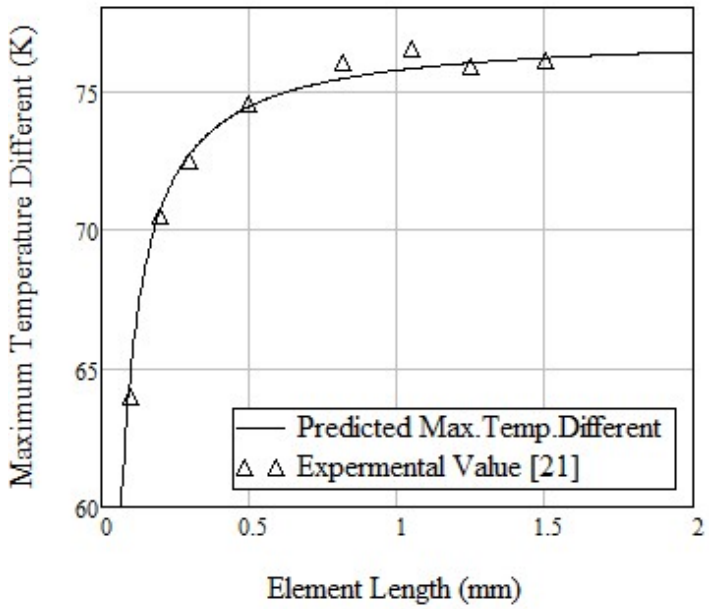

Figure 6.4 Dependence of maximum temperature difference on TE element length [21].

Furthermore, the current model is also able to predict the experimental data of the performance curves. Figure 6.5 shows cooling power as a function of temperature differences at the cold side for the AIN-based IMC04-018-02 module [21] when different current is applied. When the temperature difference is totally suppressed, the module produces cooling power of about 5 W which is identical to the power density of 80 W/cm^2 at cold junction. The analytical and experimental results of the temperature variation and cooling power shows a fair degree of coherence which justifies the modeling methodology.

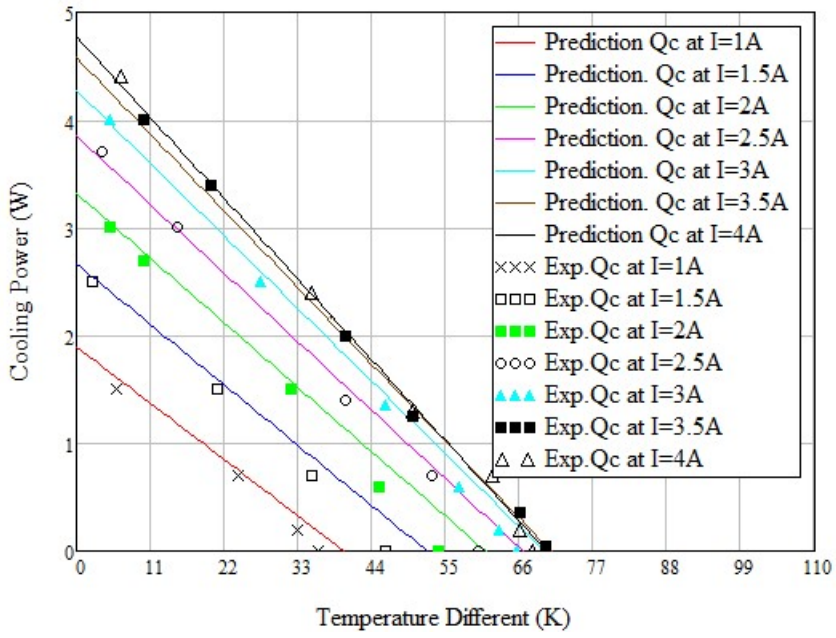

Figure 6.5 Heat load characteristics of TE micro cooler IMC04-018-02 with AlN substance [21].

Present model not only predicts the experimental data, but can predict the numerical work for a miniature device as well. The parameters input used in prediction present model and numerical data were shown in Table 6 and Table 7, which was provided by Wei Zhu's et al. [31].

Table 6 Material Properties of Thermoelectric Module [31, 36, and 42]

Parameters	Seebeck coefficient (α)	Electrical resistivity (ρ)	Thermal conductivity (k)
n-type material	$-200*10^{-6}$ (V/K)	$1*10^{-5}$ (Ω m)	1.0 (W/m K)
p-type material	$200*10^{-6}$ (V/K)	$1*10^{-5}$ (Ω m)	1.0 (W/m K)
Cooper strip	$6.5*10^{-6}$ (V/K)	$1.67*10^{-8}$ (Ω m)	400 (W/m K)

Table 7 Geometric Information [31]

Criterion	Symbols (Unit)	Values at 27 ºC
Number of thermocouples	N	1.0
Thermo-element length	l_e (mm)	0.25
Cross section of element	A_e (mm^2)	0.25
Substrate thickness	l_c (mm)	0.1

Figure (6.6) shows a good agreement between the current study and simulation data, where the cold side temperature is imposed with current applied. Because of the Peltier heat, where the cold side temperature value depends on current, the cold side temperature reduces rapidly until it reaches the optimum value of current then increased.

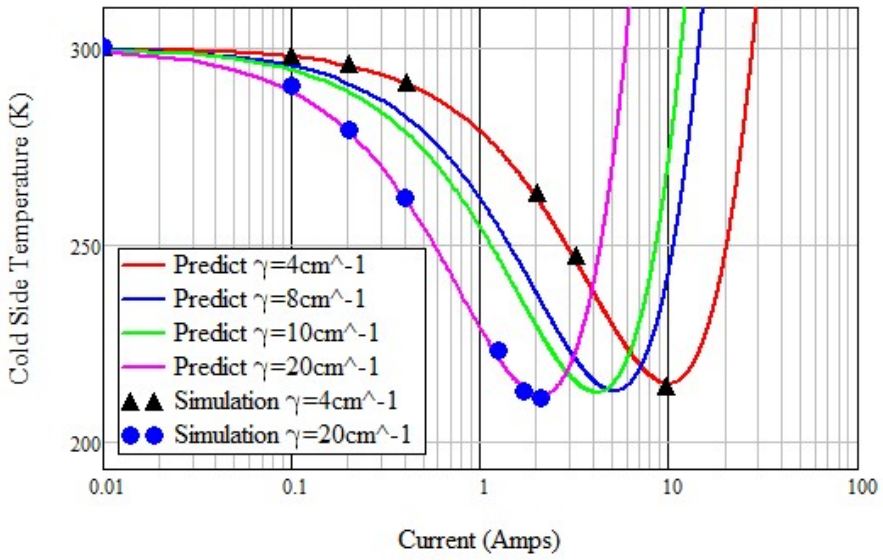

Figure 6.6 Analytical vs. simulation of the current-dependent cold-side temperature of TECs with different ratios of length to cross section area [31]

Moreover, the performance curves of the thermoelectric cooler module with the single couple was predicted as well. Figure 6.7 shows the effective geometric size on the performance of the miniature TE, where two different modules were used.

Theoretically when the cooling power increases at the cold junction of TE, temperature difference would decrease. When the cooling power increases to a particular value, the temperature difference decreases to zero, and now the cooling power is considered as maximum cooling power of TEC. Similarly, the maximum cooling temperature difference is obtained at zero cooling power. Moreover, both Q_{max} and ΔT_{max} indicate the parameters that describes the performance of TEC which cannot be achieved simultaneously. The cooling power density in Figure 6.7 increases significantly with the size decreasing. When the width of thermoelement is w=0.5 mm, power density is 35 W/cm^2 which is about four times larger than that of the TEC at w= 1 mm. Consequently, the cooling power density differs significantly when the cold-side areas of the TECs are changed.

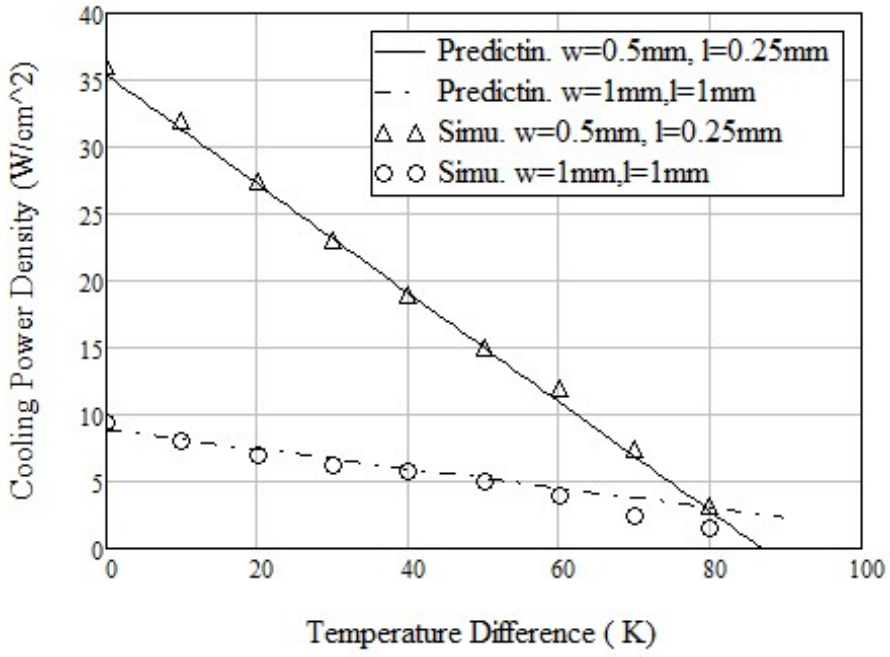

Figure 6.7 Analytical model against simulation study of the load lines of the thermoelectric models with different geometric sizes. The operating current is 3.7 A [31].

After confirm the present model with experimental and numerical data of miniature thermoelectric cooler, it can be concluded it can predict the thermoelectric generator as well. The equations from (4.5) to (4.9) are used to validate the main experimental data for commercial TEG, which consist of three types of the thermoelectric generator modules with three various of element length. The input parameters and characteristics for commercial modules are shown in Table 8 and Table 9.

Table 8 Parameters for a Thermoelectric Generator Module [25, 26]

Parameters (Symbol)	Value (Unit)	Parameters	Value (Unit)
Hot side Temperature (T_2)	300 (K)	TE element cross-section (A_e)	1.96 (mm^2)
Seebeck Coefficient (α)	$2*10^{-4}$ (V/K)	TE element high (l_e)	1.14 – 2.54 (mm)
Electrical Resistivity (ρ)	$1.1*10^{-4}$ (Ω m)	Substrate thickness (l_c)	1.0 (mm)
Thermal conductivity (k)	0.15 (W/m K)	Substrate AIN thermal conductivity (k_c)	$3*10^{-2}$ (W/m K)
Figure of merit (ZT) at 27 ºC	0.727	Electrical contact resistivity (ρ_c)	$1.1*10^{-5}$ (Ω m^2)
# of thermocouples (n)	127		

Table 9 Parameters for Commercial TE Modules (MELCOR) [25]

Modules	Element high l_e (mm)	Geometric factor A_e/l_e (mm)	conductivity ratio $r=k/k_c$	Resistivity ratio $s=\rho_c/\rho$ (mm)	Thermal conductivity for ceramic plate
CP1.4-127-10	2.54	0.771	0.096	0.1	15.6
CP1.4-127-06	1.52	1.289	0.122	0.1	12.3
CP1.4-127-045	1.14	1.719	0.104	0.1	14.4

Figure 6.8 shows the power output versus temperature difference for three of the commercial modules with variation element length, the solid line refers to analytical validation with experimental data that is referred by dots and shows a good agreement. Interestingly, that power output increases with reducing the element length of the thermoelectric TEG. Power output is about 2.5 W resulted from present model comparing with that in experimental that is about 2.0 W at 100 K when the element length is 1.14 mm. This resulting indicate to that using less materials with TEs devices produce a high-power output.

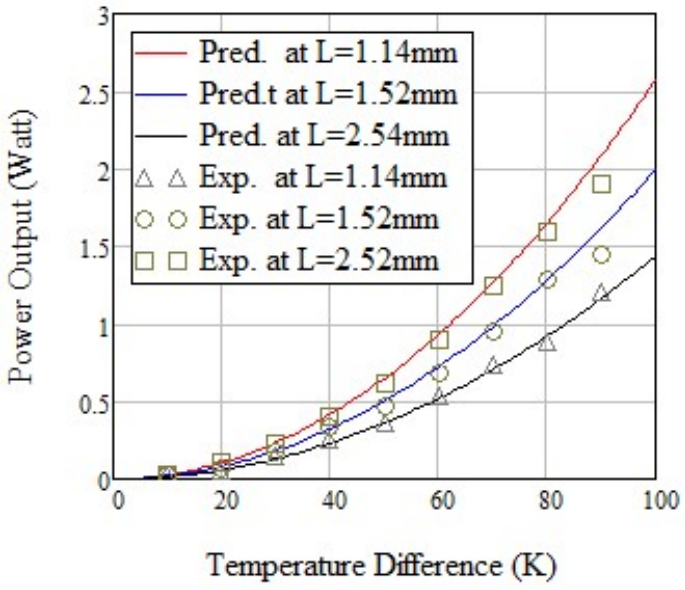

Figure 6.8 Experimental (symbols) and theoretical (solid lines) power output of thermoelectric generators as a function of temperature difference along with variation of leg length, where $\Delta T = T1 - T2$. The experimental data are adopted from the work of Min and Rowe (1992) [25, 26].

6.3 The Theoretical Results of Present Study for Miniature TECs.

After confirming the current model with some measurements of both coolers and generators, the characteristics of the both miniature and typical thermoelectric cooler are

studied in this section. It is known, the significant parameters in the thermoelectric cooler devices that should be achieved are cooling power and coefficient of performance (COP). Figure 6.9 (a) and (b) displays the analytical cooling power and COP versus current supplied for both miniature and large TEC. The parabolic curve of cooling power with current is plotted at number of the element n=36, and which yield an optimum current for particular condition of 2 and 4 Amperes which attained the best cooling and COP for both miniature and large TEC.

Miniature and large TEC shows similar performances in cooling power and COP including current, but the power density of the miniature TEC is higher than in large TEC, where power density is the division of cooling power to TEC area. This similar reflects use of the 'best fit' contact resistance used and seen to fall in the anticipated range.

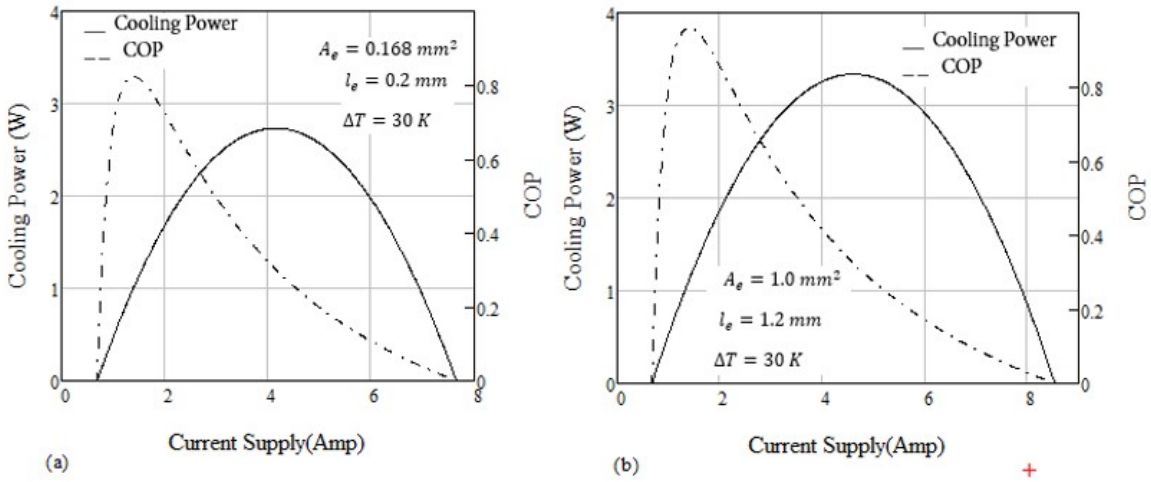

Figure 6.9 Cooling power and COP versus current supply.at ΔT = 30 K and n = 36 for (a) miniature TE cooler (b) typical TEC.

Table 10 Properties and Dimensions for the Commercial Products of the Large TE [16].

Parameter	Symbol (unit)	Value
Cross section area of element	A (mm^2)	1.0
Element length	L_e (mm)	1.2
Geometry factor	Ge (mm)	0.84
TE dimensions	W*L*H (mm*mm*mm)	30*30*3.4

6.3.1 Impact of the Element Length of Miniature TEC

This section studies how the performances respond to the change of element length of the thermoelectric cooler device along with operating current, of 2 amperes, which are shown in Figure 6.10 (a) and (b) for the miniature and macro TEC. High cooling power and coefficient of performance can be obtained at a thermo-element length about 0.2 mm and 1.2 mm, that were selected by the manufacturer (see Tables 5 and 10), for both a miniature and macro thermoelectric cooler, respectively. These two values of element length are considered as an optimal element length. Despite element length of typical module is large compared to miniature one, but they have same geometry factor, and they gave almost same values of cooling power and COP. That means that the performance of TEC and cooling power are affected by geometric factor ($G_e = A_e/l_e$), where the optimum geometry factor for both μTEC and macro TEC is used about 0.84 mm.

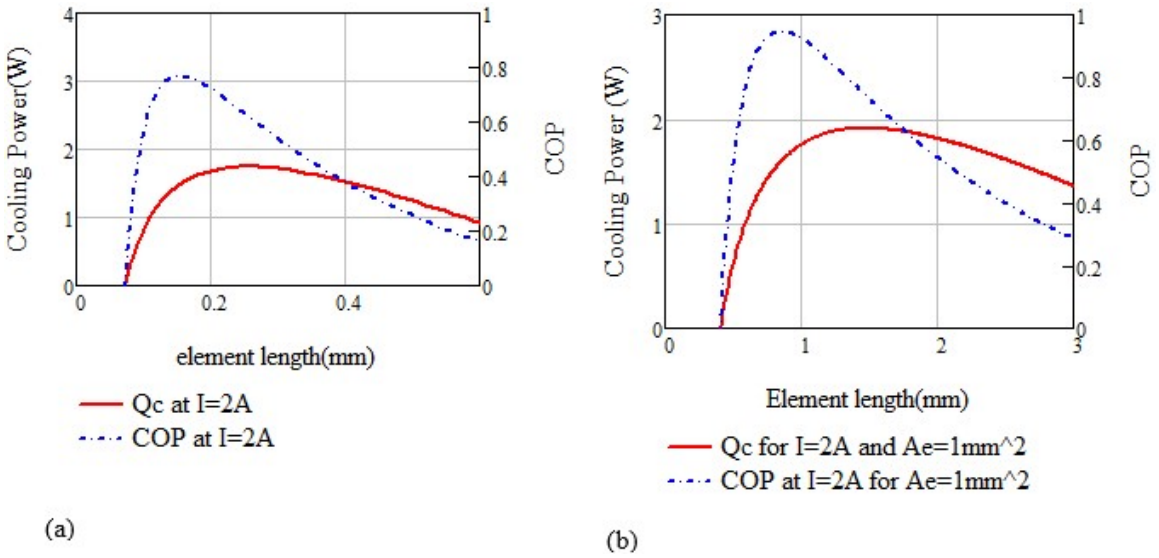

Figure 6.10 Cooling power and COP versus element length along with operating current of 2 Amperes at ΔT = 30 K. (a) A_e = 0.168 mm^2 for a micro TE cooler, and (b) A_e = 1.0 mm^2 for a large TE cooler.

6.3.2 Influence of the Substrate Material Type

Here the impact of the substrate for miniature and macro-TEC is studied for two types of materials, which are commonly used. These two kinds of materials are represented by aluminum nitride (AlN) and alumina (aluminum oxide) (Al_2O_3). The former material has thermal conductivity higher than that for the last one. Figure 6.11 (a) and (b) shows the cooling power and COP as a function of element length with two type of ceramic plates, where $r = k/k_c$. In typical TEC, the performance curves for AIN and AL_2O_3 are too close to performance curve of ideal material (s=0, r=0), therefore, the manufacturers use the cheap material that is AL_2O_3, which is not true for the μTEC.

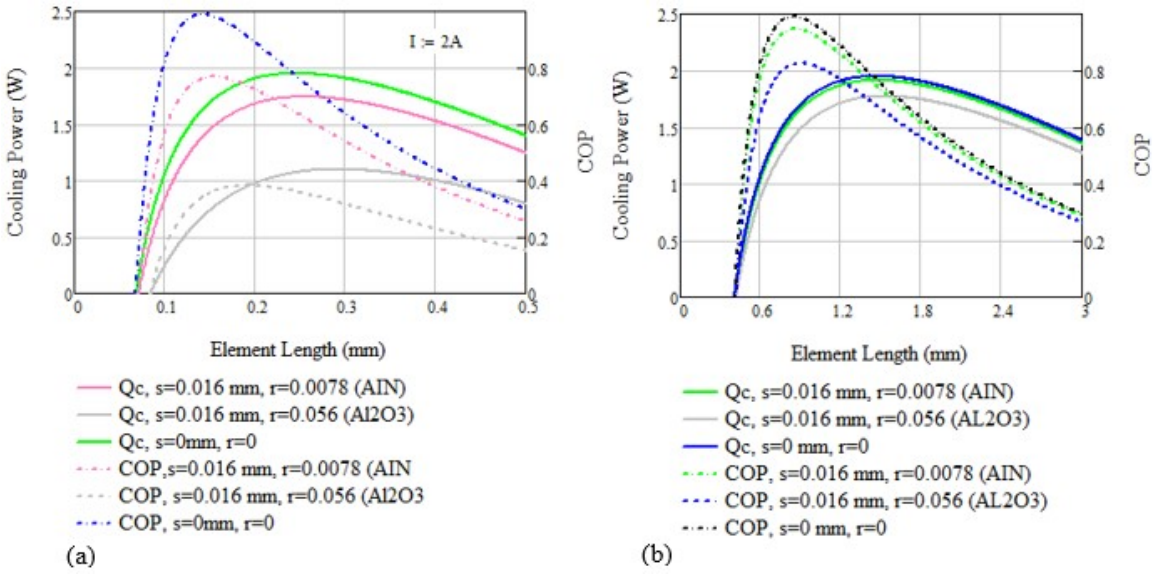

Figure 6.11 Comparison of ceramic materials between aluminum nitride (AlN) and alumina (Al2O3) in micro thermoelectric coolers, for (a) I = 2 A and Ae = 0.168 mm^2, (b) I = 2 A and Ae = 1.0 mm^2.

6.3.3 Micro and Large Thermoelectric Generators [6]

After studying the effect of thermo-element and substrate material on miniature and macro thermoelectric coolers devices, here in this section the effect load resistance is studied on thermoelectric generators. Figure 6.12 (a) and (b) compares the analytical model for power output and efficiency as a function of load resistance ratio for miniature and typical TEC. At the match load resistance (R_L/R_e =1), the maximum power output and efficiency for miniature TEC are occurred of 1.6 W and 9.7%, respectively. However, the performance of both miniature and large TEG is too close in spite of six times lower in μTEG. This indicates that using commercial TEG with less materials has a superior performance. As it is mentioned before, the power density of the μTEG is extremely higher than that of the large TEG.

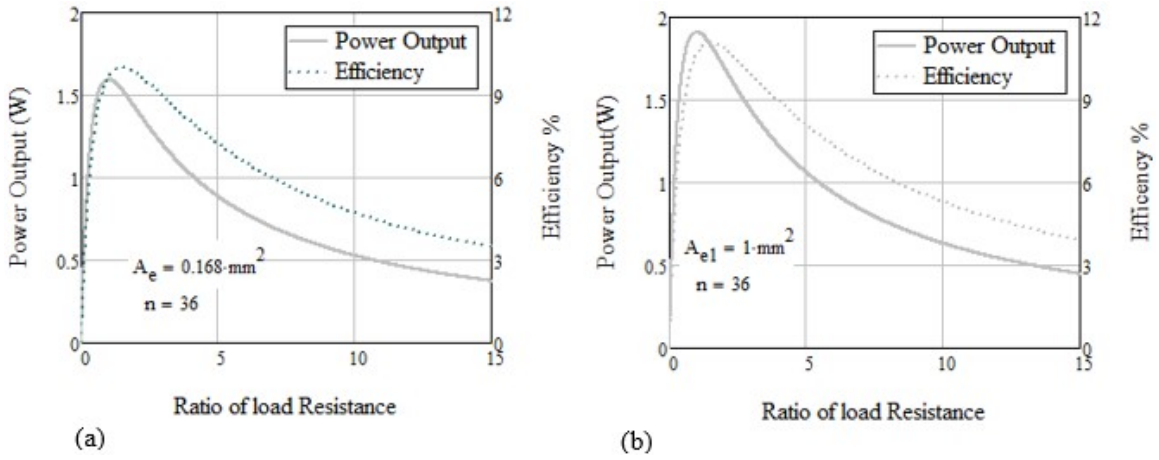

Figure 6.12 Power output and efficiency versus load resistance ratio for micro and large TE generators at ΔT = 250 K, $T2$ =300 K and n = 36, (a) Ae = 0.168 mm2 and lo = 0.2 mm for a micro TE generator, and (b) Ae = 1.0 mm2 and lo = 1.2 mm for a large TE generator. The other parameters are shown in Table 5. R_L is the load resistance and $R_e$is the internal resistance defined in Equation (4.10).

6.3.4 Effect of Element Length and Substrate Material on μTEG

The impact of both the substrate material and element length on the power output and efficiency were investigated in this section when the ratio of the load resistance R_L to internal resistance R_e is maintained at 1 . The power output and efficiency versus thermo-element length are plotted based on two types of materials of substrate which are AIN and Al_2O_3 as shown in Figure 6.13 for μTEG. It is worth mentioning that internal resistance is calculated as a function of element length, so load resistance ratio is recalculated for every change of element length. In Figure 6.13, the power output by using AIN with an element length of 0.2 mm or less, for μTEG, produces doubling value of power compared to that used alumina at same range of element length. This means that the influence substrate material is dominated, so aluminum nitride with element 0.2 mm or less should be used for miniature thermoelectric generator. The efficiency of device is increased with AIN material as well.

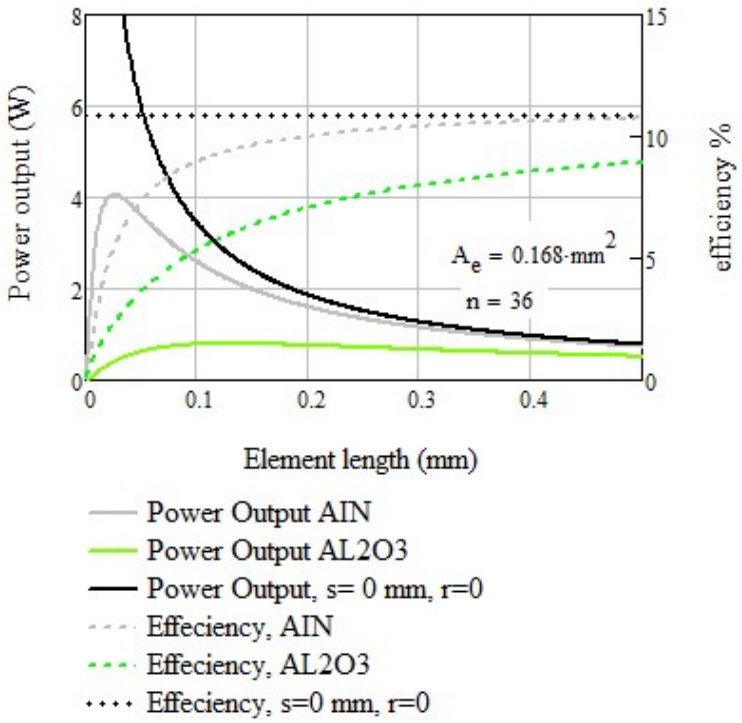

Figure 6.13 Power output and efficiency versus leg length at ΔT=250 K, T_2=300 K, R_L /R_e =1for micro TEG

6.4 Maximum Cooling Power and Maximum Current

In this section, both of maximum cooling power and maximum current for thermoelectric cooler were investigated with effect of element length. Maximum cooling power and maximum current against element length are plotted in Figure 6.14 by using equations (2.55) and (2.70). Interestingly the decreasing element length below 0.5mm leads to increase in both maximum cooling power and current, respectively. Therefore, the perfect element length to be used in the miniature thermoelectric devices is about 0.2 mm.

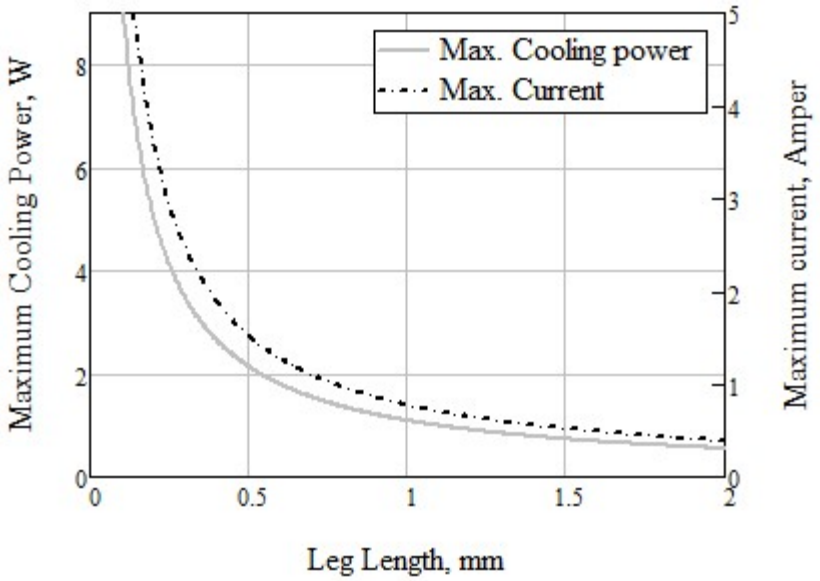

Figure 6.14 Maximum cooling power and maximum current versus element length.

6.5 Effect Minimizing Thermoelectric Devices on the Effective Material Properties

Equations from (4.15) to (4.18) were plotted as a function of element length to study the impact of miniature thermoelectric devices on the effective materials properties. Figures 6.15 and 6.16 show effective material properties (the effective figure of merit, effective Seebeck coefficient, effective electrical resistivity, and effective thermal conductivity) versus element length, where the characteristics are plain in range 0.5 mm $< l$. In the other word, the TE modules have same effective material properties when element length is bigger than 0.5 mm, while these properties are changed (not same) when element is less than 0.5 mm.

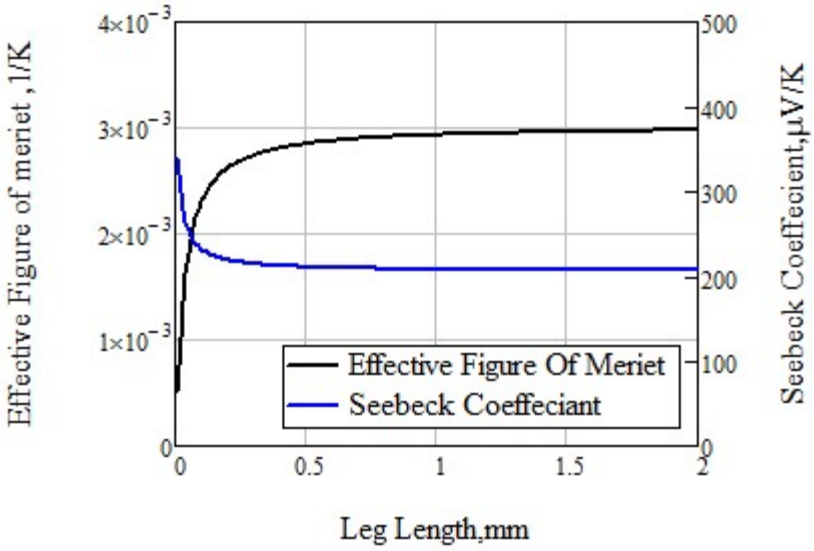

Figure 6.15 Effective figure of merit and Seebeck coefficient versus element length.

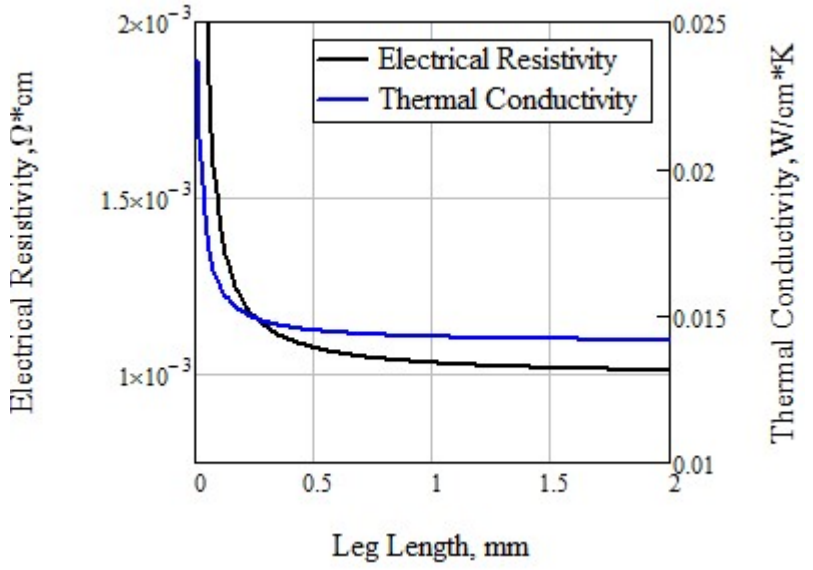

Figure 6.16 Electrical resistivity and thermal conductivity against leg length.

6.6 Experimental

Experimental data should be collected to validate the current analytical model, but there are many reasons which impede the research. Some of these reasons are: the price

of the required modules with different lengths cost about $5000 per module to be manufactured, and difficulties of controlling the sample in the stand test (because of miniature size). Furthermore, to prove current model, the intrinsic material properties for modules should be provided, but manufacturers do not provide it to consumers that also considers as a reason which also creates hindrance for the experiment.

Figure 6.17 shows cooling power of the experimental data (symbols), by using effective material properties, and the analytical model results (solid lines) as a function of temperature difference. Various current was plotted nevertheless. The results show some discrepancy between the analytical values and experimental data because of the small size of the module tested, and there were heat losses during the testing. These losses are beyond to uncontrollable on hot side temperature.

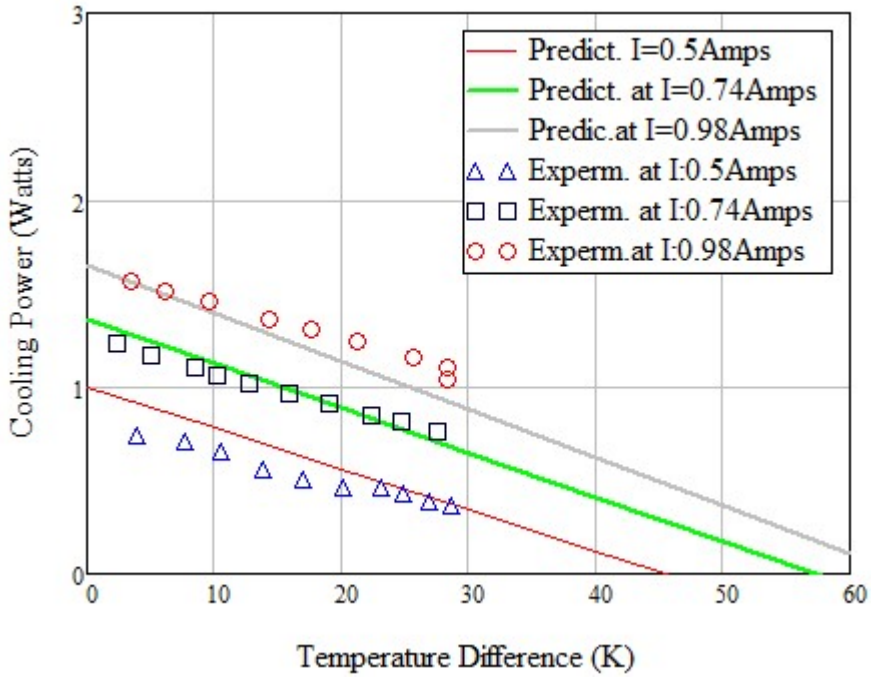

Figure 6.17 Analytical vs. experimental cooling power comparison for SP5612-01AC.

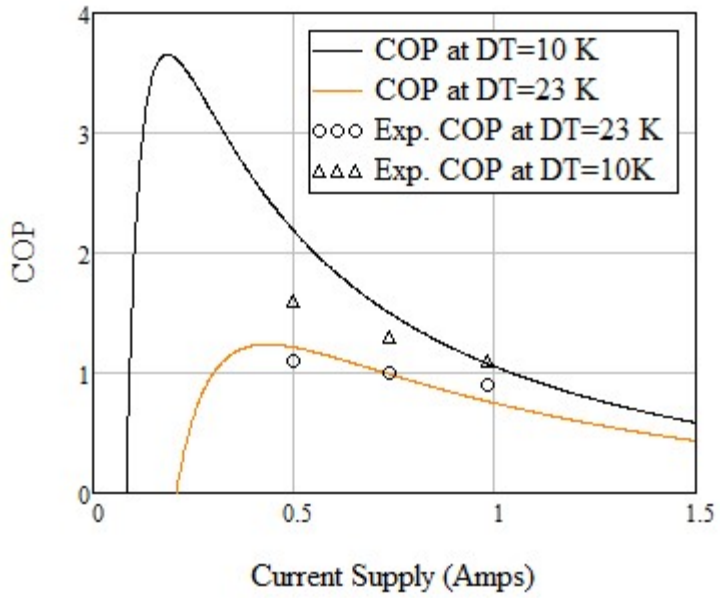

Figure 6.18 Analytical vs. experimental COP comparison for SP5612-01AC.

Figure 6.18 illustrates the experimental COP data with the predicted values. For the same reasons that are mentioned above, there are big discrepancies between the experimental and prediction data. In addition, the data collected were just for three values of current supply. When a low current of 0.2 Amps and a high current of 1.4 Amps were applied, no steady state occurs because of the micro size for module tested.

CHAPTER VII

7 CONCLUSION AND SUMMARY

The theoretical method was applied to study the effect of electrical contact resistance (that occurs at thermoelectric element and conductors). This theoretical work was built based on the ideal equations that included contact resistance. Power cooling, in the case of TECs, and power output, in the case of TEGs, are affected by reducing element length, where contact resistance has become the dominator with reducing element length. In addition, the research included studying effects of the thermoelectric dimensions such as element length, and substrates material type. Using aluminum nitride AlN substrates in the range $0.1 < l_e < 0.2\, mm$ can keep the thermoelectric cooler's efficiency at the satisfactory level. Also, this range or below 0.2 mm causes big a problem in the manufacturing because the contact resistance plays a major role in this case. Therefore, contact resistance that causes decreasing in TEC's performance was taken into account.

Interestingly, the power density of a miniature thermoelectric cooler device produced a high value of 15 W/cm^2 compared with large thermoelectric cooler that result in 0.37 W/cm^2. The analytical method validated the previous experimental work and showed a good agreement. Furthermore, effect element length on the effective material properties were studied for the miniature commercial module and validated the performance curves of the commercial module. Due to a lack of the miniature modules

required to do the experimental part and validate it with analytical study in the market, the study was limited to theoretical analysis.

REFERENCES

[1] Wu KH, Hung CI. Thickness scaling characterization of thermoelectric module for small-scale electronic cooling. J Chin Soc Mech Eng 30, pp. 475–481, 2009.

[2] Rowe DM. Thermoelectric Handbook: Macro to Nano. 1st ed. CRC, 2006.

[3] Sean Lwe Leslie Weera. Analytical Performance Evaluation of Thermoelectric Modules Using Effective Material Properties, Western Michigan University, 2014.

[4] Chen G. Nanoscale Energy Transport and Conversion. Oxford University; 2005.

[5] Gurevich YG, Logvinov GN. Physics of thermoelectric cooling. Semicond Sci Technol 20, pp. R57-R64, 2005.

[6] H. Lee, Thermal Design: Heat Sinks, Thermoelectrics, Heat Pipes, Compact Heat Exchaners, and Solar Cells. Hoboken: John Wiley & Sons, Inc., 2010.

[7] S. Kim et al., "Thermoelectric power generation system for future hybrid vehicles using hot exhaust gas," Journal of Electronic Materials, vol. 40, no. 5, pp. 778-784, 2011.

[8] V. V. Gusev, A. A. Pustovalov, N. N. Rybkin, L. I. Anatychuk. B. N. Demchuk, and I. Y. Ludchak, "Milliwatt-power radioisotope thermoleectric generator (RTG) based on plutonium-238," Journal of Electronic Materials, vol. 40, no. 5, pp. 807-811, May 2011.

[9] D. Kraemer et al., "High performance flat-panel solar thermoelectric generators with high thermal concentration," Nature, vol. 10, no. 7, pp. 532-537, July 2011.

[10] K. McEnaney, D. Kraemer, and Z. and Chen, G. Ren, "Modeling of concentrating solar theroelectric generators," Journal of Applied Physics, 2011.

[11] T. J. Seebeck, "Magnetic polarization of metals and minerals, Abhandlungen der Königlichen Akademie der Wissenschaften zu Berlin ed. Berlin, Germany, 1822.

[12] G. S. Nolas, J. Sharp, and H. J. Goldsmid, Thermoelectrics. Heidelberg, Germany: Springer, 2001.

[13] H. Alam and S. Ramakrishna, "A review on the enhancement of figure of merit from bulk to nano-thermoelectric materials," Nano Energy, vol. 2, pp. 190-212, October 2012.

[14] H. Lee, "Thermoelectrics design and materials," 2016.

[15] B. Poudel et al., "High-thermoelectric performance of nanostructured bismth antimony telluride bulk alloys," Science, vol. 320, no. 5876, pp. 634-638, May 2008.

[16] Harald Böttner et al.” New Thermoelectric Components Using Microsystem Technologies”, JOURNAL OF MICROELECTROMECHANICAL SYSTEMS, vol. 13, no. 3, June 2004.

[17] A. Attar, "Studying the Optimum Design of Automotive Thermoelectric Air Conditioning," 2015.

[18] Wei Zhu et al., Finite element analysis of miniature thermoelectric coolers with high cooling performance and short response time. Vol. 44, no. 9, pp. 860- 868, September 2013.

[19] I. Chowdhury, R. Prasher, K. Lofgreen, G. Chrysler, S. Narasimhan, R. Mahajan, D. Koester, R. Alley, R. Venkatasubramanian, On-chip cooling by superlatticebased thin-film thermoelectric, Nature Nanotechnol. 4, pp. 235- 238, 2009.

[20] B.J. Huang, C.J. Chin, C.L. Duang, A design method of thermoelectric cooler, Int. J. Refrig. 23, pp.208- 218, 2000.

[21] V. Semenyuk, "Thermoelectric Micro Modules for Spot Cooling of High Density Heat Sources," 20th International Conference on Thermoelectrics, pp. 391-396, 2001.

[22] Semenyuk, V., Miniature thermoelectric modules with increased cooling power. Proceedings of 25th International Conference of Thermoelectrics, pp. 322-326, 2006.

[23] H. Lee, "The Thomson effect and the ideal equation on thermoelectric coolers," Energy, vol. 56, pp. 61-69, 2013.

[24] E. J. Sandoz-Rosado, "Investigation and Development of Advanced Models of Thermoelectric Generators for Power Generation Applications," Rochester Institute of Technology, ,Rochester, Master Thesis UMI Number: 1469748, 2009.

[25] D. R. Gao Min, "Optisation of thermoelectric module geometry for wast heat electric power generation," *Journal of Power Sources,* vol. 38, pp. 253-259, 1992.

[26] Min, G., et al. determining the electrical and thermal contact resistance of a thermoelectric module. In 11th International Conference on Thermoelectrics, Arlington, Texas, 1992.

[27] V. Semeniouk, J. –P. Fleurial, " Novel High performance Thermoelectric Microcooler with Diamond Substrates," 16th International Conference on Thermoelectrics, 1997.

[28] D. R. G. Min, "Cooling performance of integrated thermoelectric,"Solid- State Electronics 43, pp. 923- 929, 1999.

[29] C.H. Chen, S. Y. Huang, " Development of a non-uniform-current model for predicting transient thermal behavior of thermoelectric coolers," Appl. Energy 100 , p. 326–335, 2012.

[30] Wei Zhu et al., "Finite Element Analysis of Miniature Thermoelectric Coolers with High Cooling Performance and Short Response Time," Microelectronics Journal 44, pp. 860-868, 2013.

[31] Bongkyun Jang et al., "Optimal Design for Micro-thermoelectric Generators Using Finite Element Analysis," Microelectronic Engineering 88, pp. 775-778, 2011.

[32] J. L., Pérez-Aparicio, R. Palma, R. L. Taylor, "Finite element analysis and material sensitivity of Peltier thermoelectric cells coolers," *Int. J. Heat Mass Transfer 55,* pp. 1363–1374, 2012.

[33] K. H. Lee et al., "Effect of Thermoelectric and Electrical Properties on the Cooling Performance of a Micro Thermoelectric Cooler," *Journal of Electronic Materials Journal of Elec Materi 39,* pp. 1566-571, 2010.

[34] H. Kim, O. J. Kim, K. H. Lee, M. Elimelech, "Optimal design of a microthermoelectric cooler for microelectronics," *Microelectron. J. 42,* pp. 772–777, 2011.

[35] K. H Wu, C.I. Huang, "Thickness scaling characterization of thermoelectric module for small-scale electronic cooling," *J. Chin Soc. Mech. Eng. 30,* pp. 475-481, 2009.

[36] W. H. Chen, C. Y. Liao, C. I. Hung, "A numerical study on the performance of miniature thermoelectric cooler affected by Thomson effect," *Appl. Energy 89,* pp. 464–473, 2012.

[37] L.M Goncalves, J.G. Rocha, C. Couto, P. Alpuim, J.H. Correia, On-chip array of thermoelectric Peltier microcoolers, Sens. Actuatiors A. 145-146, pp. 75-80, 2008.

[38] H. Lee, A. Attar, and S. Weera, "Performance evaluation of commercial thermoelectric modules using effective material properties," in 2014 International Conference on Thermoelectrics, Nashville, pp. 1-5, 2014.

[39] J. D'Angelo and T. Hogan, "Long term thermoelectric module testing system," Review of Scientific Instruments, vol. 80, pp. 1-3, October 2009.

[40] A. Y. Faraji and A. Akbarzadeh, "Design of a compact, portable test system for thermoelectric power generator modules," Journal of Electronic Materials, vol. 42, no. 7, pp. 1535-1541, November 2013.

[41] L. I. Anatychukl and M. V. Havrylyuk, "Procedure and equipment for measuring parameters of thermoelectric generator modules," Journal of Electronic Materials, vol. 40, no. 5, pp. 1292-1297, March 2011.

[42] E.E. Antonova, D.C. Looman, Finite elements for thermoelectric device analysis in ANSYS, in: International Conference on Thermoelectrics, Clemson, US, 2005.

APPENDIX A

NOMENCLATURE

Variable	Nomenclature	Variable	Nomenclature
$\boldsymbol{A_e}$	Cross section area of TE element (mm^2)	R	Internal resistance (Ω)
$\boldsymbol{l_e}$	TE element length (mm)	R_L	Load resistance (Ω)
$\boldsymbol{Ge}$	Geometry Factor (mm)	V	Electrical voltage (V)
COP	Coefficient of performance	Z	Figure of merit (K^{-1})
T	Temperature (K)	$\vec{E}$	Electrical field vector ($V\ m^{-1}$)
ΔT	Temperature difference (K)	$\vec{J}$	Electrical current density ($A\ m^{-2}$)
Q	Heat transfer rate (W)	$\vec{q}$	Heat flux vector ($W\ m^{-2}$)
W		n	Number of couples
I	Electrical current (Amps)	STEG	Solar Thermoelectric Generator
k	Thermal conductivity ($W\ m^{-1}\ K^{-1}$)	FEM	Finite Element Method
K	Thermal conductance ($W\ K^{-1}$)	IC	Integral Current

Greek Symbol	Nomenclature
$\boldsymbol{\alpha}$	Seebeck coefficient ($V\ K^{-1}$)
$\boldsymbol{\rho}$	Electrical resistivity (Ω cm)
η	Efficiency

$\boldsymbol{\tau}$	Thomson coefficient (V K^{-1})
$\boldsymbol{\pi}$	Peltier coefficient (W A^{-1})
$\vec{\boldsymbol{\nabla}}$	Grad, $\frac{\vartheta}{\vartheta x} + \frac{\vartheta}{\vartheta y} + \frac{\vartheta}{\vartheta z}$

Superscript	Nomenclature
$*$	Effective material properties

APPENDIX B

DATA SHET FOR MODULE TEST SP561201AC

SP5612
Single-Stage Thermoelectric Cooler
RoHS EU Compliant

TYPICAL PERFORMANCE VALUES -01AC

Specification for Module Test SP561201AC

Hot Side Temperature (°C)	27
Δ Tmax (°C-dry N2):	69
Qmax (watts):	2.0
Imax (amps):	1.4
Vmax (vdc):	2.17
AC Resistance (ohms):	1.32

MECHANICAL CHARACTERISTICS

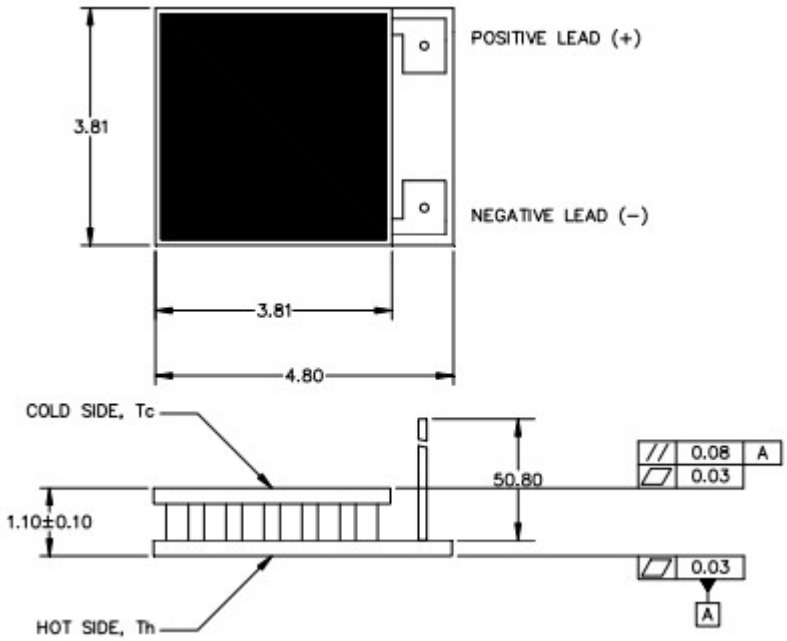

ORDERING OPTIONS PRODUCT FEATURES

Model Number	Description
SP5612-01AC	TEM, Metallized Exterior, Unsealed

PRODUCT FEATURES

Ceramic material: Aluminum Oxide.

Device exterior surface: Cu + Ni + Au Metallization.

Lead wires are 32 AWG Copper Bus, Tin Plated.

ENVIRONMENT: ONE ATMOSPHERE DRY NITROGEN